

Topology of Center Vortices¹

H. REINHARDT

Institut für Theoretische Physik

Universität Tübingen

Auf der Morgenstelle 14

D-72076 Tübingen

Abstract

The topology of center vortices is studied. For this purpose it is sufficient to consider mathematically idealised vortices, defined in a gauge invariant way as closed (infinitely thin) flux surfaces (in $D=4$ dimensions) which contribute the n^{th} power of a non-trivial center element to Wilson loops when they are n -foldly linked to the latter. In ordinary 3-space generic center vortices represent closed magnetic flux loops which evolve in time. I show that the topological charge of such a time-dependent vortex loop can be entirely expressed by the temporal changes of its writhing number.

1 Introduction

The vortex picture of confinement introduced already in the late 70s [1] has only recently received strong support from lattice calculations performed in the so-called maximum center gauge [2] where one fixes only the coset G/Z , but leaves the center Z of the gauge group G unfixed. In this gauge the identification of center vortices can be easily accomplished by means of the so-called center projection, which consists of replacing each link by its closest center element. The so obtained vortex content is a physical property of the gauge ensemble (in the sense of renormalization group invariance) [3] and produces virtually the full string tension [4]. Furthermore, the string tension disappears when the center vortices are removed from the Yang-Mills ensemble [2]. This property of center dominance of the string tension survives at finite temperature and the deconfinement phase transition can be understood in a 3-dimensional slice at a fixed spatial coordinate as a transition from a percolated vortex phase to a phase in which vortices cease to percolate

¹Supported by DFG under grant number DFG-Re856/4-1.

[5]. Furthermore, by calculating the free energy of center vortices it has been shown that the center vortices condense in the confinement phase [6]. It has also been found on the lattice that if the center vortices are removed from the gauge ensemble, chiral symmetry breaking disappears and all field configurations belong to the topologically trivial sector [7].

In $D = 4$ center vortices are closed magnetic flux sheets. In ref. [8] it was shown that the topological charge (Pontryagin index) of center vortex sheets is given by their intersection number², see also refs. [9], [10]. Based on this result the topological susceptibility was calculated for a random vortex model [11] in ref. [12] and for the center projected vortex ensemble in ref. [13].

In the present paper I study the topology of generic center vortices, which represent (in general time-dependent) closed magnetic flux loops, and express their topological charge in terms of the topological properties of these loops. I will show that the topological charge of generic center vortices is given by the temporal change of the writhing number of the magnetic flux loops.

The organisation of the paper is as follows: In sect. 2 I give a topological definition of center vortices in continuum Yang-Mills theory by means of their effect on Wilson loops and give explicit representations of the gauge potential of center vortices. In particular I construct the gauge potential of generic center vortices representing, at a fixed time, closed magnetic flux loops. In sect. 3 I discuss the various types of singular points of vortex sheets carrying non-zero topological charge, like intersection points or twisting points. In sect. 4 I express the topological charge of generic center vortex loops by their writhing number. I illustrate the obtained result by a means of an example in sect. 5. Finally a short summary and some concluding remarks are given in sect. 6.

2 Center vortices in continuum Yang-Mills theory

2.1 Definition of center vortices

In D -dimensional continuum Yang-Mills theory center vortices are localised gauge field configurations which carry flux, which is concentrated on $D = 2$ dimensional closed hypersurfaces (i.e. on closed sheets in $D=4$ dimensions or on closed loops in $D=3$ dimensions).

²Note that in 4 dimensions 2-dimensional sheets generically intersect in points.

Furthermore, their flux is quantized such that they contribute a non-trivial center element to a (large) Wilson loop in the fundamental representation, when they are non-trivially linked to the latter. To be more precise, if we assume that the flux is concentrated on the closed hypersurface $\partial\Sigma$, then we can define the gauge potential A_μ of a center vortex in D -dimensions by means of its effect on a Wilson loop by the relation

$$Pe \underset{C}{\oint}^{-\oint dx_\mu A_\mu(\partial\Sigma)} = Z^{L(C,\partial\Sigma)}, \quad (1)$$

where $A_\mu = A_\mu^a T_a$ with T_a being the generators³ of the gauge group in the fundamental representation and P denotes path ordering. Furthermore Z denotes a non-trivial center element of the gauge group and

$$L(C, \partial\Sigma) = \oint_C dx_\mu \oint_{\partial\Sigma} d^{D-2} \tilde{\sigma}_{\mu\nu} \partial_\nu^x D^{(D)}(x - \bar{x}(\sigma)) \quad (2)$$

is the linking number between the Wilson loop C and the closed vortex hypersurface $\partial\Sigma$. Here $\bar{x}_\nu(\sigma)$ denotes a parametrisation of the vortex sheet $\partial\Sigma$ with parameters $\sigma = (\sigma_1, \dots, \sigma_{D-2})$ and $d^{D-2} \tilde{\sigma}_{\mu\nu} = \frac{1}{(D-2)!} \epsilon_{\mu\nu\alpha_1 \dots \alpha_{D-2}} d^{D-2} \sigma_{\alpha_1 \dots \alpha_{D-2}}$ is the dual of the surface element

$$d^{D-2} \sigma_{\alpha_1 \dots \alpha_{D-2}} = \epsilon_{a_1 \dots a_{D-2}} \partial_{a_1} x_{\alpha_1}(\sigma) \dots \partial_{a_{D-2}} x_{\alpha_{D-2}}(\sigma), \quad \partial_{a_i} = \frac{\partial}{\partial \sigma_{a_i}}. \quad (3)$$

Furthermore, $D^{(D)}(x - \bar{x}(\sigma))$ denotes the Green function of the D dimensional Laplacian

$$-\partial^2 D^{(D)}(x) = \delta^{(D)}(x). \quad (4)$$

For the gauge group $SU(N)$ the center $Z(N)$ is given by the N different N^{th} roots of unity

$$Z(k) = e^{i\frac{2\pi}{N}k} \mathbb{1}, \quad k = 0, 1, \dots, N-1 \quad (5)$$

where $\mathbb{1}$ denotes the N -dimensional unit matrix. Like all group elements, the center elements $Z(k)$ can be represented as exponentials of Lie algebra-valued vectors

³We use antihermitean generators of the gauge group.

$$Z(k) = e^{-E(k)}, \quad E(k) = E^a(k)T_a. \quad (6)$$

Up to a factor of 2π these vectors $E(k)$ are given by the co-weights $\mu(k)$ ($E(k) = 2\pi\mu(k)$), which live entirely in the Cartan subalgebra and define the corners of the fundamental domain of the $SU(N)$ algebra. They are dual to the simple roots and satisfy the relation

$$e^{-\hat{E}(k)} = \mathbb{1}, \quad \hat{E}(k) = E^a(k)\hat{T}_a \quad (7)$$

where \hat{T}_a denotes the generators of the gauge group in the adjoint representation, $(\hat{T}_a)^{bc} = f^{bac}$.

Given the property $Z(k)^N = \mathbb{1}$, eq. (1) implies that the Wilson loop is a vortex counter mod. N . Furthermore, comparing eqs. (6) and (7) it is seen while the quarks, living in the fundamental representation, do see center vortices the gluons, living in the adjoint representation, are center blind and do not see center vortices. To gluons center vortices look like (unobservable) Dirac strings. (A center vortex has no effect on a Wilson loop in the adjoint representation).

From the definition of the center vortices (1) it is clear that the different (non-trivial) center elements $Z(k)$ (5) are associated with different types of center vortex flux. For the gauge group $SU(2)$ there is only one single non-trivial center element $Z(1) = -1$ and hence only one type of center vortices. For $SU(N > 2)$ there are $N - 1$ non-trivial center elements giving rise to $N - 1$ different center vortex fluxes. Since

$$Z(k) = Z(1)^k \quad (8)$$

fusion and fission of center vortices are possible. However, due to the relation (8) a center vortex with flux corresponding to the center element $Z(k)$ can be regarded as a bunch of k center vortices, each associated with the basic non-trivial center element $Z(1)$. For topological consideration it is therefore sufficient to consider only center vortices associated with the basic element $Z(1)$. For this reason it is also sufficient to consider the gauge group $SU(2)$, to which we will confine myself later on.

2.2 The gauge potential of center vortices

In principle, the gauge potential of a center vortex will have non-abelian components. However, since the center of a gauge group is entirely in the Cartan subgroup, one can choose the gauge potential of center vortices in the Cartan subgroup.

From the definition of center vortices (1) and the definition of the linking number (2), one can read off that a specific realisation of the gauge potential of a center vortex living on the closed hypersurface $\partial\Sigma$ is given by ($E = E(k)$)

$$a_\mu(\partial\Sigma, x) = -E \int_{\partial\Sigma} d^{D-2} \tilde{\sigma}_{\mu\nu} \partial_\nu^x D(x - \bar{x}(\sigma)) \quad (9)$$

where I have assumed the minimal flux necessary to produce in eq. (1) the desired center element. Indeed, this gauge potential represents a center vortex, whose flux

$$\mathcal{F}_{\mu\nu}(\partial\Sigma, x) = \partial_\mu a_\nu(\partial\Sigma, x) - \partial_\nu a_\mu(\partial\Sigma, x) \quad (10)$$

is entirely located on the infinitesimally thin vortex hypersurface $\partial\Sigma$

$$\mathcal{F}_{\mu\nu}(\partial\Sigma, x) = E \int_{\partial\Sigma} d^{D-2} \tilde{\sigma}_{\mu\nu} \delta^{(D)}(x - \bar{x}(\sigma)). \quad (11)$$

In this respect, this gauge potential (9) represents a mathematical idealisation of a center vortex. From the physical point of view, center vortices are extended objects, where the flux is smeared out in the transversal direction perpendicular to the vortex hypersurface $\partial\Sigma$. In other words, physical center vortices have a finite thickness. This thickness can be measured on the lattice and is obtained to be typically of the order of one fm [2]. For the present considerations, where I concentrate on the topological properties of center vortices, the finite transversal extension of these vortices is completely irrelevant. In fact, one can assume an arbitrary shape function for the transversal extension of the center vortices, which, however, drops out from the topological charge (Pontryagin index), which I am interested in here, see ref. [8]. So in the following I will use the mathematical idealisation of a center vortex gauge potential defined by eq. (9)⁴. As a side remark, I mention that this gauge potential fulfils the Lorentz gauge $\partial_\mu a_\mu(\partial\Sigma, x) = 0$ (except on $\partial\Sigma$).

⁴In **dynamical** considerations it is unavoidable to use physical vortices of finite “thickness”. This is because the mathematically idealised thin vortices have infinite Yang-Mills action, see also ref. [8]. Furthermore, thick vortices also contribute non-trivially to adjoint Wilson loops and can account for the so-called Casimir scaling [14].

Due to the fact that the linking number $L(C, \partial\Sigma)$ between a loop C and a closed surface $\partial\Sigma$ equals the intersection number

$$I(C, \Sigma) = \oint_C dx_\mu \int_\Sigma d^{(D-1)} \tilde{\sigma}_\mu \delta^{(D)}(x - \bar{x}(\sigma)) = L(C, \partial\Sigma) \quad (12)$$

between the loop C and the $D - 1$ -dimensional hypersurface (volume) Σ enclosed by the sheet $\partial\Sigma$, one can give an alternative representation for the gauge potential of an idealised center vortex in the form

$$\mathcal{A}_\mu(\Sigma, x) = E \int_\Sigma d^{D-1} \tilde{\sigma}_\mu \delta^{(D)}(x - \bar{x}(\sigma)) . \quad (13)$$

It is worth mentioning that this form of the gauge potential is precisely the continuum analogue of the gauge configurations arising on the lattice after center projection [8]. This type of vortex fields have been referred to in [8] as *ideal* center vortex, while the gauge potential defined by eq. (9) has been referred to as *thin* center vortex. While the thin vortex potential $a(\partial\Sigma, x)$ (9) manifestly depends only on the boundary $\partial\Sigma$ where the flux associated with the vortex is located, the ideal vortex gauge potential $\mathcal{A}(\Sigma, x)$ (13) is defined on the $(D - 1)$ -dimensional hypersurface Σ . For fixed boundary $\partial\Sigma$ (i.e. for fixed center vortex flux) different choices of Σ correspond to different choices of the $Z(N)$ gauge. Indeed, consider two $(D-1)$ -dimensional hypersurfaces, Σ_1 and Σ_2 , having the same boundary $\partial\Sigma_1 = \partial\Sigma_2$. Then⁵

$$\Sigma_1 \cup (-\Sigma_2) = \partial\mathcal{M} \quad (14)$$

represents the boundary of a D -dimensional hypersurface (volume) \mathcal{M} . The center gauge transformation $g(\mathcal{M}, x) \in Z(N)$ which converts $\mathcal{A}(\Sigma_1, x)$ into $\mathcal{A}(\Sigma_2, x)$ is given by

$$g(\mathcal{M}, x) = \exp(-E\chi(\mathcal{M}, x)) \quad (15)$$

where

$$\chi(\mathcal{M}, x) = \int_{\mathcal{M}} d^D \tilde{\sigma} \delta^{(D)}(x - \bar{x}(\sigma)) = \begin{cases} 1 & , \quad x \in \mathcal{M} \\ 0 & , \quad \text{otherwise} \end{cases} \quad (16)$$

⁵Here $(-\Sigma)$ denotes the hypersurface resulting from Σ by reversing its orientation.

is the characteristic function of \mathcal{M} . In fact, with (15) one has

$$\begin{aligned}\mathcal{A}_\mu(\Sigma_1, x)^{g(\mathcal{M}, x)} &\equiv g(\mathcal{M}, x) \mathcal{A}_\mu(\Sigma_1, x) g^\dagger(\mathcal{M}, x) + g(\mathcal{M}, x) \partial_\mu g^\dagger(\mathcal{M}, x) \\ &= \mathcal{A}_\mu(\Sigma_1, x) + E \partial_\mu \chi(\mathcal{M}, x) = \mathcal{A}_\mu(\Sigma_2, x),\end{aligned}\quad (17)$$

where I have used

$$\partial_\mu \chi(\mathcal{M}, x) = - \int_{\partial \mathcal{M}} d^{D-1} \tilde{\sigma}_\mu \delta^{(D)}(x - \bar{x}(\sigma)) \quad (18)$$

which follows from (16) by means of Gauss' theorem.

Since $a_\mu(\partial\Sigma, x)$ (9) and $\mathcal{A}_\mu(\Sigma, x)$ (13) both produce the same Wilson loop, they have to be gauge equivalent. In fact one can show [8] that

$$\mathcal{A}_\mu(\Sigma, x) = a_\mu(\partial\Sigma, x) + V(\Sigma, x) \partial_\mu V(\Sigma, x) \quad (19)$$

where the gauge transformation

$$V(\Sigma, x) = \exp(-E\Omega(\Sigma, x)) \quad (20)$$

is defined by the solid angle $\Omega(\Sigma, x)$ subtended by the $(D-1)$ -dimensional hypersurface Σ from the point x

$$\Omega(\Sigma, x) = \int_{\Sigma} d^{D-1} \tilde{\sigma}_\mu \partial_\mu^x D(x - \bar{x}(\sigma)). \quad (21)$$

Furthermore, one can show that the thin vortex gauge potential (9) is just the transversal part of the ideal center vortex potential (13)

$$a_\mu(\partial\Sigma, x) = P_{\mu\nu} \mathcal{A}_\nu(\Sigma, x), \quad P_{\mu\nu} = \delta_{\mu\nu} - \frac{\partial_\mu \partial_\nu}{\partial^2}. \quad (22)$$

In the following I will refer to both $a_\mu(\partial\Sigma)$ and $\mathcal{A}_\mu(\Sigma)$ as gauge potential of an (ideal and thin) center vortex since both potentials describe the same mathematically idealized, infinitesimally thin flux sheet. To distinguish between these two potentials I will refer to $a_\mu(\partial\Sigma, x)$ and $\mathcal{A}_\mu(\Sigma, x)$ as regular and singular gauge, respectively. Note that $a_\mu(\partial\Sigma, x)$ is a well behaved function of x except on the vortex sheet $\partial\Sigma$ itself, while $\mathcal{A}_\mu(\Sigma, x)$ has support only on the hypersurface Σ where it diverges.

2.3 The flux of center vortices

Whether the flux of a center vortex (11) is electric or magnetic, or both depends on the position of the $(D - 2)$ -dimensional vortex surface $\partial\Sigma$ in D -dimensional space. For definiteness let us consider a D -dimensional Euclidean space-time manifold. It is spanned by $(D - 1)$ spatial and one temporal basis vector. A vector is called *spatial* if it is spanned entirely from the spatial basis vectors. Similarly, a vector parallel to the temporal basis vector is referred to as *temporal*. In this space $(d \leq D)$ -dimensional hypersurfaces are spanned by d tangent vectors. A $(d \leq D)$ -dimensional infinitesimal hypersurface element $\delta\Sigma^{(d)}$ is spanned by d linear independent tangent vectors. If all $d(\leq (D - 1))$ tangent vectors are spatial the hypersurface element is called *spatial*, $\delta\Sigma_s^{(d)}$, if one tangent vector is temporal it is called *temporal*, $\delta\Sigma_t^{(d)}$. A hypersurface Σ completely built up from *spatial* or *temporal*, respectively, hypersurface elements is referred to as *spatial* Σ_s or *temporal* Σ_t , respectively. Note that generic vectors and hypersurfaces are neither temporal nor spatial. For definiteness let us confine ourselves in the following to $D=4$ space-time dimensions.

2.3.1 Spatial vortex surfaces

Consider a center vortex defined by a purely spatial boundary $\partial\Sigma_s$ (which is the boundary $\partial\Sigma_s$ of a purely spatial 3-dimensional volume Σ_s). It carries only electric flux, which is directed normal to the vortex surface $\partial\Sigma_s$, see Fig. 1 (a). Indeed, for a purely spatial 3-volume Σ_s the spatial component of the gauge potential vanishes

$$\vec{\mathcal{A}}(\Sigma_s, x) = 0 \quad (23)$$

as follows from eq. (13) and the definition of the dual surface element $d^3\tilde{\sigma}_\mu = \frac{1}{3}\epsilon_{\mu\alpha\beta\gamma}d^3\sigma_{\alpha\beta\gamma}$. Consequently the \vec{B} -field of such vortices vanishes. For such vortices the temporal part of the gauge potential becomes (with $d^3\tilde{\sigma}_0 = d^3x$)

$$\mathcal{A}_0(\Sigma_s, x) = E\delta(x_0 - \bar{x}_0)\chi(\Sigma_s, \vec{x}), \quad (24)$$

where \bar{x}_0 is the time instant at which the purely spatial center vortex surface $\partial\Sigma_s$ exists, and $\chi(\Sigma, \vec{x})$ is the characteristic function of the (spatial) 3-volume Σ defined by eq. (16) with $D = 3$. The gauge potential (24) gives rise to an electric field

$$\vec{E}(\partial\Sigma, x) = -\vec{\partial}\mathcal{A}_0(\Sigma, x) = -\delta(x - \bar{x}_0) E \vec{\partial}\chi_\Sigma(\vec{x}) , \quad (25)$$

which is concentrated on the spatial surface $\partial\Sigma$ and is normal to it. The purely spatial vortex surfaces $\partial\Sigma_s$ existing at a single time-instant can be considered as pathological.

The generic case will be closed vortex sheets $\partial\Sigma$ evolving in time and at a fixed time these vortex sheets represent closed loops C of magnetic flux, which is tangential to the vortex loop (see fig. 1 (b)).

2.3.2 Temporal vortex surfaces

For temporal hypersurfaces Σ_t the temporal part of the gauge potential (13) has obviously to vanish

$$\mathcal{A}_0(\Sigma_t, x) = 0 \quad (26)$$

as follows again from the property of the dual volume element $d\tilde{\sigma}_\mu$.

Consider now the spatial part $\vec{\mathcal{A}}(\Sigma_t, x)$ (13) of a center vortex in the singular gauge defined on a 3-dimensional temporal hypersurface $\Sigma_t^{(3)}$ in D=4. $\Sigma_t^{(3)}$ is swept out by the time-evolution of a 2-dimensional open surface (disc) $\Sigma^{(2)}(t)$ in ordinary 3-space \mathbb{R}^3 (see fig. 1 (b)), i.e. at a fixed time t , $\Sigma_t^{(3)}$ represents a (open spatial) disc $\Sigma_s^{(2)}(t)$. In fact, by definition, a purely temporal hypersurface contains a temporal tangent vector. Therefore one can identify one of the parameters $\sigma_{i=1,2,3}$ characterising the hypersurface $\Sigma_t^{(3)}$ in 4-dimensional space with time, e.g. $\sigma_1 = \bar{x}_0 = \bar{t}$. Using

$$\int_{\Sigma_t^{(3)}} d^3\tilde{\sigma}_k = \frac{1}{3!}\epsilon_{k\alpha\beta\gamma} \int_{\Sigma_t^{(3)}} d^3\sigma_{\alpha\beta\gamma} = \frac{1}{3!} \int d\bar{t} \int_{\Sigma^{(2)}(\bar{t})} 3\epsilon_{k0ij} d^2\sigma_{ij} = \int d\bar{t} \int_{\Sigma^{(2)}(\bar{t})} d^2\tilde{\sigma}_k, \quad (27)$$

where $d^2\tilde{\sigma}_k = \frac{1}{2}\epsilon_{kij}d^2\sigma_{ij}$, and $\delta^{(4)}(x - \bar{x}(\sigma)) = \delta(t - \bar{t})\delta^{(3)}(x - \bar{x}(t, \sigma_1, \sigma_2))$ the gauge potential of a temporal center vortex (in singular gauge) becomes

$$\mathcal{A}_k\left(\Sigma_t^{(3)}, \vec{x}, t\right) = E \int_{\Sigma_s^{(2)}(t)} d^2\tilde{\sigma}_k \delta^{(3)}(\vec{x} - \bar{x}(t, \sigma_2, \sigma_3)) . \quad (28)$$

This gauge potential (28) gives rise to a magnetic field $\vec{B} = \vec{\partial} \times \vec{\mathcal{A}}$, which by means of Stoke's theorem is obtained as

$$B_i \left(\partial \Sigma_s^{(2)}(t), \vec{x} \right) = E \oint_{\partial \Sigma_s^{(2)}(t)} dx'_i \delta^{(3)} \left(\vec{x} - \vec{x}'(\sigma) \right). \quad (29)$$

Indeed this field is directed tangential to the closed loop $\partial \Sigma^{(2)}$. Furthermore, due to its time-dependence the vector gauge potential (28) generates also an electric field

$$\vec{E} = \partial_t \vec{\mathcal{A}} \left(\Sigma_s^{(2)}, t \right) \quad (30)$$

which is normal to the surfaces $\Sigma^{(2)}(t)$.

A comment is here in order concerning the time-dependence of the open spatial disc $\Sigma_s^{(D-2)}(t)$ which during its time-evolution traces out the temporal hypersurface $\Sigma_t^{(D-1)}$. During its time-evolution $\Sigma_s^{(D-2)}(t)$ changes only near its boundary $\partial \Sigma_s^{(D-2)}(t)$ (which represents the center vortex at a fixed time t) as is illustrated for the $D = 2 + 1$ dimensional case in fig. 3: The temporal hypersurface $\Sigma_t^{(2)}$ given by the mantle of the cylinder is swept out by the time-evolution of an open (spatial) string $\Sigma_s^{(1)}(t)$ whose boundary $\partial \Sigma_s^{(1)}$ (given by its two endpoints) represents the vortex at a fixed time t . At the initial time $t = \bar{t}_i$ when the vortex(-anti-vortex-pair) is created $\Sigma_s^{(1)}(\bar{t}_i)$ is given by a single point (the position of vortex and antivortex). As the time increases $\Sigma_s^{(1)}$ becomes an open string which grows at its end points until $t = \bar{t}_f$ where it becomes a closed loop, which has no boundary and therefore carries no vortex. (The vortex disappears at $t = \bar{t}_f$). The closed spatial loop $\Sigma_s^{(1)}(t \geq \bar{t}_f)$ remains unchanged up to the time $t = \bar{t}_s$ where it merges to the spatial surface $\Sigma_s^{(2)}$. The sudden disappearance of $\Sigma_s^{(1)}(t)$ at $t = \bar{t}_s$ induces an electric field

$$\vec{E} = \partial_t \vec{\mathcal{A}} \left(\Sigma_s^{(1)}(t) \right) \quad (31)$$

which compensates the electric field

$$\vec{E} = -\vec{\partial} \mathcal{A}_0 \left(\Sigma_s^{(2)} \right) \quad (32)$$

which is carried by the spatial (hyper-)surface $\Sigma_s^{(2)}$ at its boundary $\partial \Sigma_s^{(2)} = \Sigma_s^{(1)}(\bar{t}_s)$.

2.3.3 Generic vortex surfaces

A generic 3-dimensional hypersurface Σ whose boundary $\partial\Sigma$ represents a center vortex will in general be neither purely temporal nor purely spatial. However, one can exploit the $Z(N)$ gauge freedom to split Σ into purely spatial and temporal parts

$$\Sigma = \Sigma_s \cup \Sigma_t \tag{33}$$

and, furthermore, to move the spatial part Σ_s to such a time t_s (e.g. to $t_s \rightarrow \pm\infty$) where no flux occurs. Let us illustrate this, for simplicity, in $D = 2 + 1$ dimensions where the center vortices are closed loops $\partial\Sigma^{(2)} = C$, which are the boundaries of open 2-dimensional discs $\Sigma^{(2)}$ (see fig.2). The vortex gauge potential has support only on this disc $\Sigma^{(2)}$. Generically this disc will take a position in space such that $\Sigma^{(2)}$ is neither purely temporal nor spatial, i.e. $\Sigma^{(2)} \neq \Sigma_s^{(2)} \cup \Sigma_t^{(2)}$, see fig.2(a). By performing a $Z(N)$ gauge transformation one can deform the area $\Sigma^{(2)}$ into the surface $\bar{\Sigma}^{(2)}$, (with $\partial\Sigma^{(2)} = \partial\bar{\Sigma}^{(2)}$) shown in fig.2(b), which has the shape of an open cylinder. The mantle part $\Sigma_t^{(2)}$ of this surface is temporal while its face $\Sigma_s^{(2)}$ at $t = \bar{t}_s$ is spatial, so that indeed $\bar{\Sigma}^{(2)} = \Sigma_t^{(2)} \cup \Sigma_s^{(2)}$.

Obviously, the splitting (33) of Σ into purely temporal and spatial parts can be achieved for both generic and non-generic center vortices⁶. This shows that the gauge potential of a center vortex (in singular gauge) can be chosen to satisfy the Weyl gauge $A_0 = 0$ except at a single time instant which can be chosen at will.

In the following I will assume that the $Z(N)$ gauge has been chosen such that eq. (33) is satisfied and that the spatial part Σ_s of the hypersurface Σ is shifted to a time t_s where no flux exists.

3 The topological charge of center vortices in terms of intersection points

The topology of gauge fields is characterised by the topological charge (Pontryagin index)

⁶In the $D = 2 + 1$ dimensional case considered in fig.2 a non-generic vortex would be a planar loop in a plane perpendicular to the time axis.

$$\nu[A] = -\frac{1}{16\pi^2} \text{tr} \int d^4x F_{\mu\nu} \tilde{F}_{\mu\nu} . \quad (34)$$

The field strength of an (ideal) center vortex (13) is given by eq. (11). Note that the flux of these vortices is indeed concentrated on the closed surface $\partial\Sigma$ and, furthermore, the direction of the flux is determined by the orientation of the vortex sheet $\partial\Sigma$. For definiteness, let us stick in the following to the gauge group $SU(2)$ where $E = 2\pi T_3$, $T_3 = -\frac{i}{2}\tau_3$. The generalization to $SU(N)$ is straightforward. Inserting (11) into the expression for the Pontryagin index (34) and using $\text{tr}(EE) = -2\pi^2$ one finds [8]

$$\nu[\mathcal{A}(\Sigma)] = \frac{1}{4} I(\partial\Sigma^{(3)}, \partial\Sigma^{(3)}) , \quad (35)$$

where

$$I(S_1, S_2) = \frac{1}{2} \int_{S_1} d\sigma_{\mu\nu} \int_{S_2} d\tilde{\sigma}'_{\mu\nu} \delta^{(4)}(\bar{x}(\sigma) - \bar{x}(\sigma')) \quad (36)$$

is the oriented intersection number of two 2-dimensional (in general open) surfaces S_1, S_2 in R^4 . Generically, two 2-dimensional surfaces intersect in R^4 at isolated points. Obviously, the (self-)intersection number $I(\partial\Sigma, \partial\Sigma)$ receives contributions only from those points $\bar{x}(\sigma) = \bar{x}(\sigma')$, where the intersecting surface patches give rise to four linearly independent tangent vectors (otherwise $d\sigma_{\mu\nu} d\tilde{\sigma}'_{\mu\nu} = 0$). Such points are referred to as singular points. One can distinguish two principally different types of singular points:

1. transversal intersection points, for which $\bar{x}(\sigma) = \bar{x}(\sigma')$ and $\sigma \neq \sigma'$,
2. twisting points, for which $\bar{x}(\sigma) = \bar{x}(\sigma')$ and $\sigma = \sigma'$.

Transversal intersection points arise from the intersection of two different surface patches while twisting points occur on a single surface patch (see sect. 5 for more details). Transversal intersection points yield a contribution ± 2 to the (oriented) intersection number $I(\partial\Sigma, \partial\Sigma)$, where the sign depends on the relative orientation of the two intersecting surface pieces. (One should note that each transversal intersection point actually contributes twice to the self-intersection number). For orientable (and oriented) closed surfaces twisting points can be turned into (a smaller number of) transversal intersection

points by surface deformation. In this sense for closed surfaces in $D = 4$ the number of transversal intersection points is even, so that the topological charge of orientable center vortex surfaces is indeed integer-valued. However, for closed oriented surfaces the oriented self-intersection number eq. (36) vanishes. Hence, vortices carrying non-zero topological charge are given by non-oriented surfaces, where the orientation defines the direction of the flux. Non-oriented vortex surfaces consist of open oriented surface patches S_i ($i = 1, 2, \dots$). The expression for the field strength eq. (11) remains valid for open surface patches and hence also for non-oriented vortex sheets.

Using eq. (11) for an oriented open surface patch S one finds upon using Stokes' theorem that the monopole current

$$j_\mu(\partial S, x) = \partial_\nu \tilde{\mathcal{F}}_{\mu\nu}(S, x) = E \oint_{\partial S} d\bar{x}_\mu \delta^{(4)}(x - \bar{x}) \quad (37)$$

flows at the boundary ∂S of the vortex patch S . The magnetic charge m of the monopole is obtained by integrating the current (37) over the 3-dimensional volume Σ dual to the monopole trajectory ∂S . This yields

$$m = E \int_{\Sigma} d\Sigma_\mu \oint_{\partial S} \delta x_\mu \delta^{(4)}(\bar{x}(\Sigma) - x) = EI(\Sigma, \partial S), \quad (38)$$

where we have used the definition of the intersection number $I(\Sigma, \partial S)$ (36), which, by the choice of Σ , is equal here to one. Hence the magnetic charge of the monopole flowing at the boundary of an oriented vortex patch is given by E (6). In view of eq. (6) we call this monopole a center monopole.

Consider a non-oriented center vortex sheet $\partial\Sigma$ which consists of two oriented patches S_1 and S_2 (see fig. 3). Since S_1 and S_2 are oppositely oriented and form together a closed surface, they possess the same boundary $\partial S_1 = \partial S_2$. Hence the two magnetic monopole loops flowing along ∂S_1 and ∂S_2 , respectively, (each with charge E) add up coherently to form the trajectory of a magnetic monopole with twice the charge of a center monopole. In view of $e^{-2E} = 1$ this monopole is a Dirac monopole whose magnetic charge is in accord with Dirac's quantization condition. Hence a magnetic (Dirac) monopole with magnetic charge $2E$ flows at the boundary between two oppositely oriented patches of a (globally non-oriented) center vortex. Thus non-oriented vortex sheets necessarily carry magnetic (Dirac) monopoles.

Indeed, a non-oriented vortex surface $\partial\bar{\Sigma}$ can be interpreted as an oriented vortex surface $\partial\Sigma$ covered with an (open) oppositely oriented Dirac sheet S_D , $\partial\bar{\Sigma} = \partial\Sigma + S_D$. The Dirac sheet S_D carries twice the flux of a center vortex, and thus, if it is oppositely oriented to the vortex surface $\partial\Sigma$, it will reverse the orientation of the latter. Furthermore the boundary of the Dirac sheet represents the world line of a Dirac monopole (here with magnetic charge $2E$). Thus non-oriented closed magnetic vortex sheets consist of oriented surface patches joined by magnetic monopole loop currents. The magnetic monopole currents change the orientation of the center vortices and are thus absolutely necessary for a non-vanishing topological charge of center vortices, see ref. [8] for more details.

The orientation of - and thus the magnetic monopole loops on - the center vortices are, however, not relevant for the confining properties of the latter, which are entirely determined by their linking properties with the Wilson loop, see eq. (1). This can be seen by noticing that non-oriented vortex surfaces differ from oriented ones by open Dirac sheets which do not affect Wilson loops.

A final comment is in order: Eq. (11) still applies to the field strength of non-oriented vortex sheets $\partial\bar{\Sigma}$. However, the field strength of non-oriented vortex sheets cannot be generated from a globally defined Abelian gauge potential. Indeed the flux of the open Dirac sheet (converting the oriented vortex into the non-oriented one) cannot be represented as the curvature of an Abelian gauge potential. The monopole current at the boundary of the Dirac sheet violates the Abelian Bianchi identity $\partial_\mu \tilde{\mathcal{F}}_{\mu\nu} = 0$, which holds for any field strength constructed from a regular Abelian gauge potential. Furthermore, though eq. (11) applies also to non-oriented vortex sheets and includes in particular the flux of the involved Dirac string it does not contain the magnetic field of the monopole itself. This might at first sight seem disturbing but in fact is a very welcome feature mimicking the non-Abelian nature of magnetic monopoles in Yang-Mills theory. This can be understood as follows. In Yang-Mills theory the magnetic monopoles arise as gauge fixing defects in the so-called Abelian gauges where one fixes only the coset G/H leaving the Cartan subgroup H unfixed. To be more precise if $V \in G/H$ is the gauge transformation $A \rightarrow A^V = VAV^\dagger + V\partial V^\dagger$ necessary to bring the gauge field into the desired Abelian gauge, the magnetic monopoles arise in the Abelian part of the induced gauge potential $\mathcal{A} = V\partial V^\dagger$. As shown in ref. [15], (see also ref. [16]) the Abelian field strength $f_{\mu\nu}^n = \partial_\mu \mathcal{A}_\nu^n - \partial_\nu \mathcal{A}_\mu^n$ (\mathcal{A}^n denotes the Abelian part of \mathcal{A}) contains the magnetic monopole with a Dirac string attached to it. Now the crucial point is that the Abelian part of the

commutator $[\mathcal{A}_\mu, \mathcal{A}_\nu]^n$ contains the same, but oppositely directed monopole field (i.e. the corresponding anti-monopole field), however, without the Dirac string, so that in (the Abelian part of) the total field strength

$$\begin{aligned} F_{\mu\nu} [V\partial V^\dagger]^n &= f_{\mu\nu}^n + [\mathcal{A}_\mu, \mathcal{A}_\nu]^n \\ &= \left(V (\partial_\mu \partial_\nu - \partial_\nu \partial_\mu) V^\dagger \right)^n \end{aligned} \quad (39)$$

the monopole does not show up while the Dirac string is left. In fact the total field strength vanishes (as it should for a pure gauge) except at the Dirac sheet, where V is singular. Thus, the total field strength, eq. (39), contains only the flux of the Dirac sheet.

The conclusion from the above considerations is that Dirac sheets (without monopole fields) naturally arise in the total field strength of non-Abelian gauge fields and are induced by the singular gauge transformations necessary to implement the Abelian gauges. This observation is consistent with the picture advocated in ref. [18]: As function of space-time-coordinates the non-Abelian gauge field changes smoothly and gradually in color space. Abelian gauge fixing rotates the gauge field as much as possible into the Abelian direction. The flux is, of course, not changed during the gauge fixing and hence still smooth. Upon Abelian projection the regions interpolating between positive and negative Abelian flux directions appear as magnetic monopoles. The monopoles are an artifact of the Abelian projection and do not show up in the full non-Abelian flux. The full non-Abelian field strength can, however, contain string like fluxes: Dirac sheets (strings) or center vortices, which may be interpreted as half Dirac sheets.

4 Topology of generic center vortices

4.1 The topological charge of generic center vortices

As is well known the topological density can be expressed as a 4-dimensional divergence

$$-\frac{1}{16\pi^2} \text{tr} F_{\mu\nu} \tilde{F}_{\mu\nu} = \partial_\mu K_\mu \quad (40)$$

where

$$K_\mu = -\frac{1}{8\pi^2}\epsilon_{\mu\alpha\beta\gamma}\text{tr}\left[A_\alpha\partial_\beta A_\gamma + \frac{2}{3}A_\alpha A_\beta A_\gamma\right] \quad (41)$$

is the topological current. For simplicity let us choose the singular gauge (13), (28) where the gauge potential of a (closed) center vortex sheet $\partial\Sigma$ has support on an (open) 3-dimensional volume $\Sigma^{(3)}$ in the 4-dimensional space-time manifold. As shown in sect.2 $\Sigma^{(3)}$ can be chosen to be the sum of a purely spatial part $\Sigma_s^{(3)}$ (existing only at a single time instant), and a purely temporal part $\Sigma_t^{(3)}$, which at a fixed time t represents a 2-dimensional open (spatial) disc $\Sigma_s^{(2)}(t)$. Since $\Sigma_s^{(3)}$ and $\Sigma_s^{(2)}$ are both localised objects in ordinary 3-space $M = \mathbb{R}^3$ the topological current $K_\mu(\vec{x}, t)$ is a localised function of the spatial coordinates which vanishes for $|\vec{x}| \rightarrow \infty$. Hence by applying Gauss' law we obtain

$$\int_M d^3x \partial_i K_i(x) = \oint_{\partial M} d\tilde{\sigma}_i(x) K_i(x) = 0. \quad (42)$$

This relation is not spoiled for non-oriented vortex sheets in the presence of magnetic monopole loops on the vortex sheets. For a generic center vortex sheet, at a fixed time, the monopole loop represents the positions of a monopole and an anti-monopole. At large distance the magnetic monopole -anti-monopole pair produces a magnetic dipole field, which drops off sufficiently rapid not to contribute to the surface term (42).

With (42) the topological charge (34) becomes

$$\nu = \int d^4x \partial_0 K_0 = \int dx_0 \partial_0 S_{CS}[A](x_0) \quad (43)$$

where

$$S_{CS}[A](x_0) = \int d^3x K_0[A](x_0, \vec{x}) \quad (44)$$

is the Chern-Simons action.

If we assume that our space-time manifold extends over a finite time interval, saying from t_i to t_f , one would naively expect that the topological charge becomes

$$\nu = S_{CS}[A](t_f) - S_{CS}[A](t_i). \quad (45)$$

This is the well-known expression for the topological charge in Weyl gauge $A_0 = 0$, in which gauge fields are considered to be smooth. However, although the gauge potential of center vortices can be chosen to satisfy the Weyl gauge (except at a single time instant, see sect.2), depending on the gauge configurations under consideration, their Chern-Simons action need not to be differentiable in the whole time interval, but may jump at intermediate time instants, say $\bar{t}_k, k = 1, 2, \dots$, which we will refer to as *singular time instants*⁷. Each of these jumps contributes to the topological charge

$$\Delta\nu = \Delta S_{CS}^{(k)} = \lim_{\varepsilon \rightarrow 0} (S_{CS}(\bar{t}_k + \varepsilon) - S_{CS}(\bar{t}_k - \varepsilon)) \quad (46)$$

These discontinuities in the Chern-Simons action will be investigated for center vortices in more detail further below, see sects. 4.2 and 5.

4.2 The Chern-Simon action of center vortices

The ideal center vortices considered above live in the Cartan subgroup. Consequently for these configurations the Chern-Simons action reduces to the Abelian one

$$S_{CS}[A](t) = \frac{1}{8\pi^2} \int d^3x \mathbf{A} \cdot \mathbf{B} \quad (47)$$

where $\mathbf{B} = \vec{\partial} \times \mathbf{A}$ denotes the magnetic field of the vortex. For a generic center vortex describing a magnetic flux loop $C(t)$ which evolves in time, the magnetic field is given by (29). Inserting this expression into eq. (47) and using the vortex gauge potential in the singular gauge (28) for $A_i(x)$ we immediately obtain for the Chern-Simon action of a generic center vortex $C(t) = \partial \Sigma_s^{(2)}(t)$ evolving in time

$$S_{CS} [A [\Sigma_s^{(2)}(t)]] = \frac{1}{4} I (\Sigma_s^{(2)}(t), C) \quad (48)$$

where

⁷The idealised center vortices which I consider in the present work can be thought of as arising by center projection from initially smooth gauge field configurations. It is the center projection which introduces the singularities.

$$I(\Sigma, C) = \int_{\Sigma} d^2 \tilde{\sigma}_i \oint_C dx_i \delta^{(3)}(x - \bar{x}(\sigma)) \quad (49)$$

is the intersection number between the open 2-dimensional surface Σ and the loop C in \mathbb{R}^3 . This intersection number $I(\Sigma, C)$ equals the Gaussian linking number $L(\partial\Sigma, C)$ between the boundary $\partial\Sigma$ of the surface Σ and the loop C , which is defined for two closed loops in \mathbb{R}^3 by

$$\begin{aligned} L(C_1, C_2) &= -\varepsilon_{ijk} \oint_{C_1} dx_i \oint_{C_2} dx'_j \partial_k D^{(3)}(x - x') \\ &= \frac{1}{4\pi} \oint_{C_1} dx_i \oint_{C_2} dx'_j \varepsilon_{ijk} \frac{x_k - x'_k}{|\vec{x} - \vec{x}'|^3}. \end{aligned} \quad (50)$$

(Note that for $\vec{x} \rightarrow \vec{x}'$ the integrand (including the measure) does not diverge but vanishes). With $I(\Sigma, C) = L(\partial\Sigma, C)$ we obtain from eq. (48) for the Chern-Simons action of a generic center vortex loop $C(t)$.

$$S_{CS}[A[C(t)]] = \frac{1}{4}W(C) \quad (51)$$

where $W(C)$ is the writhing number of the closed (time-dependent) vortex loop $C(t)$, which is defined as the coincidence limit

$$W(C) = L(C, C) \quad (52)$$

of the Gaussian linking number. In view of equations (43) and (51) we find that the topological charge of an (idealised) generic center vortex, representing a time dependent closed magnetic flux loop $C(t)$, is given by

$$\nu = \frac{1}{4} \int dt \partial_t W(C(t)). \quad (53)$$

Let us again assume that our space-time manifold has a finite extension in time direction, i.e. extends from an initial time t_i to a final time t_f . According to eq. (53) the topological charge is given by the changes of the writhing number during the evolution from the initial

time $t = t_i$ to the final time $t = t_f$. If $W(t)$ changes continuously during the whole time evolution the topological charge is given by

$$\nu = \frac{1}{4} (W(t_f) - W(t_i)), \quad (54)$$

so we need not to consider any smooth change of $W(t)$ during the time evolution in the calculation of the topological charge, which then solely depends only on the initial and final values of $W(t)$. However, the writhing number $W(t)$ may change in a discontinuous way, e.g. when two line segments of the vortex loop intersect (see below). These discontinuous changes (due to singular changes in the vortex loop), which also contribute to eq. (53), are left out in eq. (54).

If we denote by $\bar{t}_k, k = 1, 2, \dots; t_i < \bar{t}_k < t_f$ the intermediate time instants where $W(t)$ jumps by a finite amount

$$\Delta W(\bar{t}_k) = \lim_{\varepsilon \rightarrow 0} [W(\bar{t}_k + \varepsilon) - W(\bar{t}_k - \varepsilon)] \quad (55)$$

the complete expression for the topological charge for a generic center vortex is given by

$$\nu = \frac{1}{4} \left[W(t_f) + \sum_k \Delta W(\bar{t}_k) - W(t_i) \right] \quad (56)$$

This relation will be illustrated in sect. 5 by means of an example.

4.3 The self-linking number, the writhing number and the twist

Since the topological charge of generic center vortices is completely determined by the temporal changes of the writhing number, see eq. (53), let us recall some of its properties. The writhing number is defined as coincidence limit of the Gaussian linking number, see eq. (52). However, unlike the Gaussian linking number $L(C_1, C_2)$ of two closed loops C_1, C_2 the writhing number $W(C)$ is not a topological invariant, but depends on the precise shape of the loop C . In particular it is not integer but real-valued.

For a single loop C one can define the integer-valued, topologically conserved self-linking number as the Gaussian linking number between the loop C under consideration and a loop C' arising by displacing the original loop C by an infinitesimal amount ε parallel to

a unit vector $\hat{n}(\vec{x}, t)$, which has to be always orthogonal to the loop C . This displacement introduces a so-called framing of the loop by which the latter becomes a band or a ribbon bounded by C and C' (c.f. fig. 9, below). The self-linking number defined by

$$SL(C, \hat{n}) = \lim_{\varepsilon \rightarrow 0} L(C, C' = C + \varepsilon \hat{n}) \quad (57)$$

is frame dependent but integer-valued (since it represents the linking number of C and C'). Taking the coincidence limit $\varepsilon \rightarrow 0$ one finds

$$SL(C, \hat{n}) = W(C) + T(C, \hat{n}) \quad (58)$$

where $W(C)$ is the writhing number defined above by eqs. (52) and (50) and

$$T(C, \hat{n}) = \frac{1}{2\pi} \oint_C ds \frac{\vec{r}'(s)}{|\vec{r}'(s)|} (\dot{\hat{n}}(s) \times \hat{n}(s)) \quad (59)$$

is the so-called “twist”. The latter represents the integrated torsion of the ribbon bounded by C and C' . Furthermore $\vec{r}'(s)$ denotes a parametrisation of the loop C . The twist $T(C, \hat{n})$ can take any real value and also depends on the framing. Let us emphasise, while the self-linking number $SL(C, n)$ and the twist $T(C, \hat{n})$ are framing dependent, their difference, the writhing number $W(C)$, is independent of the chosen framing. Furthermore $W(C)$ and $T(C, \hat{n})$ can take any real value, but their sum $SL(C, n)$ is integer valued though framing dependent. Since the self-linking number is integer-valued and $W(C)$ is frame independent, eq. (58) implies that changing the framing can change the twist (torsion) only by an integer.

As already mentioned above, the writhing number $W(C)$ is a continuous function of the shape of the curve C but it is not a topological invariant. From its definition, eqs. (52), (50), immediately follows that $W(C)$ vanishes for planar loops C , for which the integrand in eq. (50) vanishes identically. More generally, $W(C)$ vanishes for curves possessing a symmetry plane. In this sense the writhing number measures the left-right asymmetry of a loop, i.e. its chirality. Furthermore, $W(C)$ suffers discontinuities when two segments of the loop C pass through each other: When two line segments cross (i.e. intersect) (see fig. 4 (a)) $W(C)$ changes by ± 2 , where the sign depends on the relative orientation of the crossing line segments. Furthermore, what is not commonly known and will be

demonstrated later on when we consider explicit examples, when two half-line segments cross, see fig. 4 (c), which can be interpreted as a twist (see sect. 5), the writhing number changes by $\Delta W = 2 \cdot \frac{1}{2} \cdot \frac{1}{2} = \frac{1}{2}$. Analogously, when one half-line crosses with a full line (see fig. 4 (b)) the writhing number changes by $\Delta W = 2 \cdot 1 \cdot \frac{1}{2} = 1$. All these properties of the writhing number will explicitly show up in the next section where we analyse the distribution of topological charge of a specific center vortex configuration.

5 Analysis of a lattice center vortex configuration in continuum Yang-Mills theory

5.1 The topological charge of lattice center vortices

On the lattice, idealised center vortices are co-closed hypersurfaces built up from plaquettes which are equal to a non-trivial center element. In addition these vortex surfaces have to be endowed with an orientation, which defines the direction of the vortex flux. The topological charges of such vortex hypersurfaces can in view of eq. (35), in principle, be easily determined by measuring the (oriented) intersection number: The topological charge at a lattice site x is obtained by counting all pairs of dual plaquettes⁸ meeting at the lattice site considered, i.e. one finds for the topological charge ν_x of lattice site x [12]

$$\nu_x = \frac{1}{32} N_x, \quad (60)$$

where N_x is the number of pairs of dual plaquettes meeting at site x . As discussed above, we can basically distinguish two types of singular points of vortex sheets contributing to the topological charge: transversal intersection points and twisting points. On the lattice a transversal intersection point corresponds to a site x where two mutually dual planar vortex patches, each consisting of four plaquettes meeting at x , intersect. Thus $N_x = 4 \times 4 = 16$ pairs of dual vortex plaquettes meet at a transversal intersection point, yielding $\nu_x = \frac{1}{2}$, in agreement with the continuum result (see sect. 3 and ref. [8]). A twisting point at lattice site x consists of a single (non-planar) surface segment twisting around x in such a way to produce a non-zero contribution to the intersection number. Such a surface segment is composed by plaquettes which meet at x and which can be

⁸The dual $\tilde{P}_{\mu\nu}$ of a plaquette $P_{\mu\nu}$ is defined as usual by $\tilde{P}_{\mu\nu} = \frac{1}{2}\epsilon_{\mu\nu\alpha\beta}P_{\alpha\beta}$.

connected by proceeding along plaquettes which share a link [12]⁹. For twisting points $N_x < 16$ holds. Obviously on the lattice the topological charge at a site x , see eq. (60), can take only integer multiples of $\frac{1}{32}$ since N_x is integer valued.

To illustrate the various singular vortex points, let us consider as an example the center vortex configuration shown in fig. 5. [12], which could arise in a lattice simulation after center projection, ref. [17], or in a random vortex model [11]. This vortex surface is orientable. For simplicity let us also assume that its flux is indeed oriented, so that there are no magnetic monopole loops on this vortex sheet. The total topological charge of this configuration then vanishes, $\nu = 0$. Nevertheless this configuration has various spots of non-zero topological charge [12]. There is a transversal intersection point at the intermediate time¹⁰ $n_0 = 2$ contributing $\frac{1}{2}$ to the topological charge ν . At this time there are also two twisting points at the front and back edges of the configuration each contributing $-\frac{1}{8}$ to ν . Further twisting points occur at the initial ($n_0 = 1$) and final ($n_0 = 3$) times, each contributing $-\frac{1}{8}$ to ν so that the total topological charge vanishes ($\nu = 0$) for this vortex configuration, indeed.

5.2 The writhing number of center vortex loops

Let us now interpret the same configuration as a time dependent vortex loop in ordinary 3-dimensional space (like in a movie-show) eliminating lattice artifacts due to the use of a discretised time. As illustrated in fig. 6 purely spatial vortex patches are lattice artifacts. They represent the discrete time step approximation to continuously evolving (in time) vortex loops. Fig. 7 shows the time-evolution of a closed magnetic vortex loop in ordinary 3-dimensional space which on the 4-dimensional lattice gives rise to the configuration shown in fig. 5. For simplicity we have kept the cubistic representation in $D = 3$ space, so that the loop consist of straight line segments C_i defined in fig. 8. At an initial time $t = \bar{t}_i$ an infinitesimal closed vortex loop is generated which then grows (i.e. continuously evolves) up to a time $t = \bar{t}_1$. Then the loop segment C_5 moves towards,

⁹In ref. [12] twisting points were referred to as writhing points, since in a pictorial sense, the vortex surface writhes similar to the winding of a screw. However, from a mathematical point of view it makes sound sense to refer to them as twisting points. This is because, these points can change both the writhing number and the twist, while the intersection points change only the writhing number but never the twist, as we will illustrate later.

¹⁰We quote here the time $t = n_0 a$ in (integer) units n_0 of lattice spacing a .

and at time $t = \bar{t}_2$ crosses the segment C_1 , and continues to move up to a time $t = \bar{t}_3$. After this time the loop decreases continuously and at the fixed time $t = \bar{t}_f$ shrinks to a point. In the following we calculate the topological charge of this time dependent vortex configuration by applying eq. (56).

For simplicity let us choose $t_i < \bar{t}_i$ (the birth of the vortex loop) and $t_f > \bar{t}_f$ (the death of the vortex loop). Then

$$W(t_i) = W(t_f) = 0 \quad (61)$$

since there are no vortex loops at the initial and final times. In the above field configuration shown in fig. 7 there are discontinuous changes of the vortex loop, and accordingly of the writhing number, at the creation (birth) of the vortex loop at $t = \bar{t}_i$, at the intermediate time \bar{t}_2 , where two line segments cross and two lines turn by 180 degrees, and at the annihilation (death) of the vortex loop at $t = \bar{t}_f$. Hence the topological charge of this configuration is given by (assuming $t_i < \bar{t}_f$ and $t_f > \bar{t}_f$)

$$\nu = \frac{1}{4} [\Delta W(\bar{t}_f) + \Delta W(\bar{t}_2) + \Delta W(\bar{t}_i)] \quad (62)$$

For calculational simplicity let us assume that from its creation at \bar{t}_i until the time \bar{t}_1 the vortex loop does not change its shape, but merely scales in size. The same will be assumed for the vortex evolution from \bar{t}_3 until its annihilation at \bar{t}_f . Then the change of the writhing number at vortex creation and at annihilation, respectively, is given by (with $W(\bar{t}_i - \epsilon) = 0, W(\bar{t}_i + \epsilon) = W(\bar{t}_1), W(\bar{t}_f + \epsilon) = 0, W(\bar{t}_f - \epsilon) = W(\bar{t}_3)$)

$$\Delta W(\bar{t}_i) = W(\bar{t}_1), \quad \Delta W(\bar{t}_f) = -W(\bar{t}_3), \quad (63)$$

so that we obtain for the topological charge (62)

$$\nu = \frac{1}{4} [W(\bar{t}_1) + \Delta W(\bar{t}_2) - W(\bar{t}_3)]. \quad (64)$$

The writhing numbers $W(\bar{t}_1), W(\bar{t}_3)$ are explicitly evaluated in Appendix A. One finds

$$W(\bar{t}_1) = \frac{1}{2}, \quad W(\bar{t}_3) = -\frac{1}{2} \quad (65)$$

As already stated above, a further singular change of the vortex loop shown in fig. 7 occurs at the intermediate time $t = \bar{t}_2$. Since the writhing number $W(C)$ is a unique function of the shape of the loop C (independent of any framing) the changes of W at $t = \bar{t}$ are obviously given by

$$\Delta W(\bar{t}_2) = W(\bar{t}_3) - W(\bar{t}_1) = -1 \quad (66)$$

Let us now investigate how this contribution arises from the various singular points at $t = \bar{t}_2$. At this time the line segment C_5 intersects (crosses) the line segment C_1 (see fig. 7). The crossing of these two line segments at $t = \bar{t}_2, (x, y, z) = (0, 0, 0)$ corresponds in $D=4$ to the transversal intersection point shown in fig. 5 at $n_0 = 2$. In fact, in Appendix A it is shown that the crossing of the line segments C_5 and C_1 gives rise to a change in the writhing number of

$$\Delta W(\bar{t}_2)^{(i)} = -2 \quad (67)$$

which in view of eq. (56) is in accord with the finding [8] that a transversal intersection point contributes $\Delta\nu = \pm\frac{1}{2}$ to the topological charge. Furthermore, when the loop segment C_5 crosses C_1 the paths C_4 and C_6 reverse their directions, which can be interpreted as twisting C_4 and C_6 by an angle π around the x-axis at $x = \pm a$ and at $t = \bar{t}_2$, see figs. 7, 8. In the $D = 4$ dimensional lattice realization of the present center vortex shown in fig. 5 these twistings of the vortex loop segments (in $D = 3$) by angle π correspond to the two twisting points at $n_0 = 2$ at the front and back edges of the configuration. Thus we observe that twisting points of 2-dimensional vortex sheets in $D = 4$ may manifest themselves as rotations of loop segments (here by an angle π) in $D = 3$. Hence we will refer to the turning points $(\pm a, 0, 0)$ of the rotations at $t = \bar{t}_2$ also as twisting points.

As shown in Appendix A the two twisting (turning) points $(\pm a, 0, 0)$ at $t = \bar{t}_2$ both change the writhing number by

$$\Delta W(\bar{t}_2)^t(\pm a) = \frac{1}{2} \quad (68)$$

and hence contribute $\Delta\nu = \frac{1}{8}$ to the topological charge, again in agreement with the analysis of ν in $D = 4$.

The change of the writhing number by $\Delta W = \frac{1}{2}$ by the twisting points at $(\pm a, 0, 0)$ can be easily understood by noticing that the twisting points can be interpreted as the crossing of two half-lines (see fig. 4 (c)) which changes the writhing number by only $\frac{1}{2} \cdot \frac{1}{2} = \frac{1}{4}$ of the change of $W(C(t))$ at a true intersection point of two (full) lines ($\Delta W^i = \frac{1}{2}$) so that

$$\Delta W^t = \frac{1}{2} \cdot \frac{1}{2} \Delta W^i = \frac{1}{8}. \quad (69)$$

Thus at the time $t = \bar{t}_2$ the total change in writhing number is given by

$$\begin{aligned} \Delta W(\bar{t}_2) &= \Delta W^i(\bar{t}_2) + W^t(\bar{t}_2, a) + \Delta W^t(\bar{t}_2, -a) \\ &= -2 + \frac{1}{2} + \frac{1}{2} = -1 \end{aligned} \quad (70)$$

This is in agreement with our previous result found in eq. (66). Hence one finds for the total change in the writhing number during the whole time-evolution of the vortex

$$\begin{aligned} \Delta W &= W(\bar{t}_1) + \Delta W(\bar{t}_2) - W(\bar{t}_3) \\ &= \frac{1}{2} - 1 + \frac{1}{2} = 0 \end{aligned} \quad (71)$$

which corresponds to vanishing Pontryagin index.

In view of the relation (56) the above results are in complete agreement with the contributions of the various singular points to the Pontryagin index obtained in $D = 4$ from the previous analysis of the intersection number of the vortex sheet shown in fig. 5.

5.3 The twist of the center vortex loops

Let us also consider the twist or torsion (59) of these vortex loops. For this purpose we have to introduce a framing of these loops, see fig. 9. The twist is evaluated in Appendix B. One finds

$$T(\bar{t}_1) = -\frac{1}{2}, \quad T(\bar{t}_3) = \frac{1}{2}. \quad (72)$$

This result for the twist can be also immediately read off from the framing: Consider for example the framing of the vortex loop at $t = \bar{t}_3$ shown in fig. 9(b). As one moves along

the loop, the ribbon of the framing does not twist along C_1 and C_2 . Along the path C_3 the ribbon twists by an angle $-\frac{\pi}{2}$, which, in view of eq. (59), results in a contribution $\left(-\frac{1}{4}\right)$ to the torsion $T(C)$. Along C_4 the ribbon accumulates a twist (angle) of $\frac{\pi}{2}$ i.e. a torsion $T(C_4) = \frac{1}{4}$. Furthermore the ribbon does not twist along C_5 , but accumulates a torsion of $\frac{1}{4}$ along C_6 and also along C_7 while the ribbon does not twist along C_8 . Therefore we obtain for the total twist

$$\begin{aligned} T(C(\bar{t}_3)) &= T(C_3) + T(C_4) + T(C_6) + T(C_7) \\ &= -\frac{1}{4} + \frac{1}{4} + \frac{1}{4} + \frac{1}{4} = \frac{1}{2}. \end{aligned} \quad (73)$$

This result agrees with that of the explicit calculation given in Appendix B. By the identity (58) the results for W and T imply that the self-linking number of the framed curve $C(\bar{t}_3)$ shown in fig. 9 (b) vanishes.

Let us now consider the change of the twist at $t = \bar{t}_2$. Obviously, assuming the framings adopted above, which are shown in fig. 9 (a), (b), the total change of the twist at $t = \bar{t}_2$ is given by

$$\Delta T(\bar{t}_2) = T(\bar{t}_3) - T(\bar{t}_1) = \frac{1}{2} - \left(-\frac{1}{2}\right) = 1. \quad (74)$$

Let us now investigate how this change of the twist is distributed over the various singular points at $t = \bar{t}_2$.

It is easy to see that the intersection point of C_1 and C_5 at $(x, y, z) = (0, 0, 0)$ and $t = \bar{t}_2$ does not change the twist. This is because the line segments C_1 and C_5 do not contribute to the twist at both $t = \bar{t}_1 < \bar{t}_2$ and $t = \bar{t}_3 > \bar{t}_2$ since the framing vector $\hat{n}(s)$ does not change along these line segments (see also the explicit calculations in Appendix B). The change of twist at $t = \bar{t}_2$ entirely arises from the twisting points at $(x, y, z) = (\pm a, 0, 0)$ due to the reflection of the line segments C_4 and C_6 at the $x - z$ -plane. Indeed, we could carry out the change of the vortex loop at $t = \bar{t}_2$ in two steps: First we could deform the line segment C_5 such that it intersects the line segment C_1 keeping the boundary points of C_5 fixed (see fig. 10 (a)), so that the line segments C_4 and C_6 remain unchanged. This intersection of C_5 and C_1 would still change the writhing number by $\Delta W(t_2)^{(i)} = -2$ but at the same time leave the torsion unchanged (since C_5 and C_1 do not contribute to T). Second, to produce the vortex configuration at $t = \bar{t}_2 + \varepsilon, \varepsilon > 0$ we deform the line segment C_5 to its final form by reflecting the end points of C_5 at the $x - z$ -plane, which

will also reflect the line segments C_4 and C_6 (including their framings) see figs. 10 (b), (c). This second change of the vortex loop does not only change the writhing number, namely by $\Delta W (\bar{t}_2)^t (a) + \Delta W (\bar{t}_2)^t (-a) = \frac{1}{2} + \frac{1}{2} = 1$ as discussed above, but also the twist.

One easily convinces oneself that in the second step only the sign of the twists along C_4 and C_6 changes. This can be seen as follows. The reflection at the $x-z$ -plane reverses only the sign of the y -component of a vector (while the x - and z -components are unchanged). The vectors $\hat{n}(s), \dot{\hat{n}}(s)$ of the framing along C_4 and C_6 are parallel to $x-z$ -plane and are consequently not changed by the reflection at the $x-z$ -plane. Thus also $\hat{n}(s) \times \dot{\hat{n}}(s)$ (which is an axial vector) does not change although it is parallel to the y -axis. What changes in the second step is the sign of the y -component of the vector $\vec{r}(s)$. Thus the integrand in the twist (59), and hence the twists along C_4 and C_6 themselves, change the sign:

$$\begin{aligned} T(C_4((\bar{t}_2 - \varepsilon)) &= -\frac{1}{4} \Rightarrow T(C_4(\bar{t}_2 + \varepsilon)) = +\frac{1}{4}, \\ T(C_6(\bar{t}_2 - \varepsilon)) &= -\frac{1}{4} \Rightarrow T(C_6(\bar{t}_2 + \varepsilon)) = +\frac{1}{4}. \end{aligned} \quad (75)$$

Consequently each of the twisting points at $(x, y, z) = (0, 0, 0)$ change the twist by $\Delta T = +\frac{1}{2}$, so that the total change of the twist at $t = \bar{t}_2$ is $\Delta T = 1$. This property justifies the name “twisting point”. Twisting points change not only the writhing number by $|\Delta W| < 2$ but, depending on the framing, may also change the twist, while intersection points change the writhing number by $|\Delta W| = 2$ without changing the twist. In view of eq. (58) the intersection points change also the self-linking number by $\Delta SL = \Delta W = \pm 2$.

In fig. 9 (a) and (b) the framings of the vortex loops at $t = \bar{t}_1$ and $t = \bar{t}_3$ have been chosen in such a way that the framing of the line-segment C_5 does not change as C_5 moves from $y = -a$ to $y = a$ thereby intersecting C_1 at $y = 0$. As discussed above, with these framings during the evolution from $t = \bar{t}_1$ to $t = \bar{t}_3$ the writhing number changes from $W(\bar{t}_1) = \frac{1}{2}$ to $W(\bar{t}_3) = -\frac{1}{2}$ and the twist changes from $T(\bar{t}_1) = -\frac{1}{2}$ to $T(\bar{t}_3) = \frac{1}{2}$ so that the self-linking number remains unchanged. The ribbons of the framings at both $t = \bar{t}_1, \bar{t}_3$ shown in fig. 9 (a), (b) have vanishing self-linking numbers.

To illustrate the frame-independence of the writhing number and the frame-dependence of the twist and of the self-linking number let us choose the alternative framing of the

vortex loop at $t = \bar{t}_1$ shown in fig. 9 (c). With this framing the twist of the vortex loop at $t = \bar{t}_1$ is $T(\bar{t}_1) = \frac{1}{2}$ while the writhing number is still $W(\bar{t}_1) = \frac{1}{2}$, as it should since W is framing-independent. The ribbon of the framing at $t = \bar{t}_1$ (shown in fig. 9 (c)) is now a twisted band with the self-linking number $SL(\bar{t}_1) = 1$. We can now turn the framed vortex configuration at $t = \bar{t}_1$ shown in fig. 9 (c) into the one at $t = \bar{t}_3$ shown in fig. 9 (b) by rotating the yoke (C_4, C_5, C_6) (including the corresponding framing) around the x-axis by angle π . During this process the twist does not change i.e. $T(\bar{t}_1) = T(\bar{t}_3) = \frac{1}{2}$ but the writhing number changes as in the previous case from $W(\bar{t}_1) = \frac{1}{2}$ to $W(\bar{t}_3) = -\frac{1}{2}$. Accordingly the self-linking number changes from $SL(\bar{t}_1) = 1$ to $SL(\bar{t}_3) = 0$.

In sect. 4 I have shown that only discontinuous changes in the writhing number (during the time evolution) of the vortex loop contribute to the topological charge. (Continuous changes are fully taken into account by the initial and final value of the writhing number, i.e. by $(W(t_f) - W(t_i))$, see eq. (56).) When the yoke (C_4, C_5, C_6) is rotated by an angle π around the x -axis the writhing number changes continuously except at the time when C_5 crosses (the end of) C_1 . This represents a crossing of the “full” line C_5 with the “half-line” C_1 (see fig. 4 (b)) which changes the writhing number by $\Delta W = -1$. Furthermore when C_5 crosses C_1 the vortex loop is planar so that its writhing number vanishes. Thus when C_5 intersects C_1 the writhing number changes from $W = \frac{1}{2}$ to $W = -\frac{1}{2}$ in accord with our previous findings. Note that in the present case the total change of the writhing number comes from the “half-intersection” point $(0, 0, a)$ of C_5 and C_1 which, in fact, is a twisting point. There are no further twisting points in this case since there are no further singular changes of the vortex loop. Note also when C_5 passes C_1 (keeping the framing fixed) the twist does not change, $\Delta T = 0$, but the self-linking number changes by $\Delta SL(C) = 1$, in agreement with our previous findings.

5.4 Non-oriented center vortices

As discussed in sect. 3 center vortex sheets with non-zero topological charge are necessarily non-oriented and carry magnetic monopole loops at the interface between vortex patches of different orientations. One can convince oneself that the above given analysis of the topological charge of generic center vortices in terms of the writhing number remains valid for non-oriented vortices, i.e. in the presence of magnetic monopoles. On a (non-oriented) generic vortex sheet the monopole loops evolve in time (like the vortex sheet) and show up at a fixed time on the vortex loop as monopole-anti-monopole pairs. Both monopole and

anti-monopole change the direction of the flux of the vortex loops. The writhing number depends not only on the shape but also on the orientation of the loops and fully accounts also for the topology of generic non-oriented center vortices as we will now demonstrate explicitly.

For this purpose we convert the oriented center vortex shown in fig. 5 into a non-oriented one by putting a magnetic monopole loop in the $z - t$ -plane. The time-evolution of this non-oriented vortex in the continuum is illustrated in fig.11, which is the counter part of fig.7. For calculational simplicity we have chosen the monopole loop as follows: At time t'_1 with $\bar{t}_1 < t'_1 < \bar{t}_2$ a magnetic monopole-antimonopole pair is created at $z = 0$. Monopole and antimonopole then run away from each other until they reach the positions $z = a$ and $z = -a$, respectively, at a time t''_1 with $t'_1 < t''_1 < \bar{t}_2$. Then monopole and anti-monopole keep their position in space up to a time t''_2 with $\bar{t}_2 < t''_2 < \bar{t}_3$ and subsequently approach each other until they annihilate at a time t'_2 with $t''_2 < t'_2 < \bar{t}_3$.

The presence of the monopole-antimonopole pair on the vortex loop does not give rise to additional singular changes of the writhing number as function of the time. However, the magnetic monopoles have reversed the orientation of (the relevant part of) the line segment C_1 (see figs. 8, 11) for times $t \in [t''_1, t''_2]$ and thus in particular at time $t = \bar{t}_2$ when C_1 crosses C_5 . We therefore expect that the contribution of the intersection (crossing) point at $t = \bar{t}_2, (x, y, z) = (0, 0, 0)$ to the change of the writhing number $\Delta W(t_2)^i(0)$ (see eq. (67)) has opposite sign for the non-oriented vortex. Indeed, the contribution of the intersection point is given by (see Appendix A, eq. (93)):

$$\Delta W(\bar{t}_2)^i(0) = 4 \lim_{b \rightarrow 0} L(C_1, C_5), \quad (76)$$

where $L(C_1, C_5)$ is the Gaussian linking integral for open paths defined by eq. (79) in Appendix A and b denotes the distance of the line-segment C_5 from the x -axis. Changing the orientation of C_1 changes the sign of $L(C_1, C_5)$ and in view of eq. (67) we obtain

$$\Delta W(\bar{t}_2)^i(0) = 2. \quad (77)$$

The changes of the writhing number due to the two twisting points at $t = \bar{t}_2, (x, y, z) = (\pm a, 0, 0), \Delta W(\bar{t}_2)^t(\pm a)$, do not receive contributions from the line segment C_1 and are hence not changed by the addition of the magnetic monopoles on C_1 . Hence we find for the change of the writhing number at $t = \bar{t}_2$

$$\begin{aligned} \Delta W(\bar{t}_2) &= \Delta W(\bar{t}_2)^i(0) + \Delta W(\bar{t}_2)^t(a) + \Delta W(\bar{t}_2)^t(-a) \\ &= 2 + \frac{1}{2} + \frac{1}{2} = 3. \end{aligned}$$

The writhing numbers of the vortex loop at $t = \bar{t}_1, \bar{t}_3$ are not changed by the addition of the monopole loop since the latter does not exist at these times. Thus for the non-oriented center vortex shown in fig. 11 the total change of the writhing number during the time evolution of the vortex is given by

$$\begin{aligned} \Delta W &= W(\bar{t}_1) + \Delta W(\bar{t}_2) - W(\bar{t}_3) \\ &= \frac{1}{2} + 3 + \frac{1}{2} = 4 \end{aligned}$$

which, in view of eq. (56), corresponds to a Pontryagin index $\nu = 1$. Thus the non-oriented center vortex shown in fig. 11 is topologically equivalent to an instanton.

A final remark is in order: In the above investigation of non-oriented center vortices we have tacitly extended the writhing number to non-oriented loops. In fact, since the writhing number, as well as the twist and the Gaussian self-linking number, are defined by loop integrals, these quantities can be straightforwardly generalised to non-oriented loops. One should, however, be aware that for non-(globally) oriented loops the self-linking number (57), (50) is not necessarily a topological invariant and the relation (58) need not to hold.

6 Summary and conclusions

In the present paper we have studied the topological properties of center vortices. The topological charge of center vortices is given by (a quarter of) their self-intersection number, which, however, vanishes for closed oriented vortex sheets. Topologically non-trivial vortex sheets are not globally oriented but consist of oriented vortex patches, which are joined by magnetic monopole loops. These monopole loops are irrelevant for the confining properties of center vortices as measured by their contributions to the Wilson loop but absolutely crucial for their topological properties.

The intersection number of vortex sheets receives contributions from two types of singular points: transversal intersection points, contributing $\pm\frac{1}{2}$ to the topological charge, and twisting points which give contributions of modulus smaller than $\frac{1}{2}$.

In ordinary 3-space, generic center vortices represent (in general time-dependent) closed magnetic flux loops. I have shown that the topological charge of these center vortices can be entirely expressed by the change of the writhing number of the vortex loops during the time-evolution. I have also demonstrated that transversal intersection points of the 2-dimensional vortex sheet in D=4 correspond to a crossing of two line segments of the vortex loop in D=3. Furthermore the twisting points of the vortex sheets in D=4 show up as rotations and, in particular, reflections of line segments of the vortex loop in D=3. I believe that the present analysis of the topological properties of center vortices in terms of the writhing number of time-dependent flux loops in D=3 is more transparent, although not necessarily computationally simpler, than the analysis of the self-intersection number of closed vortex sheets in D=4.

Acknowledgements:

The author is grateful to M. Engelhardt for useful discussions, in particular, on the center vortex configuration shown in fig.5., and to J. Gattnar for preparing the tex files of the other figures. He also acknowledges discussions with T. Tok.

Appendix A: Calculation of the writhing number

In the following we calculate the changes in the writhing number of the vortex configuration shown in fig. 7. We begin by calculating the writhing number of the final field configuration at $t = \bar{t}_3$. For later convenience we will, however, start by calculating the writhing number of the slightly generalised loop configuration C shown in fig. 8. This loop C has a cubistic form. It consist of straight line segments $C_i, i =, \dots, 8$, which are prallel to one of the Cartesian coordinate axis and are a distance a apart form the latter, except for the line segment C_1 , which sits on the z -axis, and the line segment C_5 , which has a distant b form the x -axis. For $b = a$ the loop C reduces to the vortex configuration at $t = \bar{t}_3$ shown in fig. 7.

It is convenient to break the loop C into the straight line segments C_i , i.e. $C = \bigcup_{i=1}^8 C_i$. The writhing number is then given by

$$W(C(b)) = L(C, C) = \sum_{i,j=1}^8 L(C_i, C_j) \quad (78)$$

where

$$L(C_i, C_j) = \frac{1}{4\pi} \int_{C_i} (d\vec{x} \times \int_{C_j} d\vec{x}') \cdot \frac{(\vec{x} - \vec{x}')}{|\vec{x} - \vec{x}'|^3} \quad (79)$$

is the Gaussian linking integral for open paths C_i . Due to the cross product the integrand obviously vanishes when the two-line segments are parallel, i.e. $d\vec{x} \parallel d\vec{x}'$, so that $L(C_i, C_i) = 0$. Since furthermore $L(C_i, C_j) = L(C_j, C_i)$, we obtain

$$W(C) = 2 \sum_{i < j} L(C_i, C_j). \quad (80)$$

By the same argument pairs of parallel paths do not contribute, for example $L(C_2, C_5) = 0$. Furthermore, the integrand, containing the product $(d\vec{x} \times d\vec{x}') \cdot (\vec{x} - \vec{x}')$, vanishes when the three vectors $d\vec{x}, d\vec{x}', (\vec{x} - \vec{x}')$ are in the same plane. This happens for any two pairs of paths within the following sets of paths $(C_1, C_2, C_3, C_7, C_8), (C_4, C_5, C_6), (C_3, C_4), (C_6, C_7)$. Thus the only non-vanishing contributions to the writhing number are given by

$$\begin{aligned} W(C) &= 2[L(C_1, C_4) + L(C_1, C_5) \\ &+ L(C_1, C_6) + L(C_2, C_4) + L(C_2, C_6) \\ &+ L(C_3, C_5) + L(C_3, C_6) + L(C_4, C_7) \\ &+ L(C_4, C_8) + L(C_5, C_7) + L(C_6, C_8)]. \end{aligned} \quad (81)$$

Since the paths C_i are all parallel to one of the coordinate axes, we use the corresponding Cartesian-coordinates to parametrise these paths

$$\begin{aligned}
C_1 : \vec{r} &= z\vec{e}_z, & \int_{C_1} d\vec{r} &= \vec{e}_z \int_{-a}^a dz, \\
C_2 : \vec{r} &= x\vec{e}_x + a\vec{e}_z, & \int_{C_2} d\vec{r} &= \vec{e}_x \int_0^a dx, \\
C_3 : \vec{r} &= -a\vec{e}_x + z\vec{e}_z, & \int_{C_3} d\vec{r} &= \vec{e}_z \int_y^0 dz, \\
C_4 : \vec{r} &= -a\vec{e}_x + y\vec{e}_y, & \int_{C_4} d\vec{r} &= \vec{e}_y \int_0^b dy, \\
C_5 : \vec{r} &= x\vec{e}_x + b\vec{e}_y, & \int_{C_5} d\vec{r} &= \vec{e}_x \int_{-a}^a dx, \\
C_6 : \vec{r} &= a\vec{e}_x + y\vec{e}_y, & \int_{C_6} d\vec{r} &= \vec{e}_y \int_b^0 dy, \\
C_7 : \vec{r} &= a\vec{e}_x + z\vec{e}_z, & \int_{C_7} d\vec{r} &= \vec{e}_z \int_0^{-a} dz, \\
C_8 : \vec{r} &= x\vec{e}_x - a\vec{e}_z, & \int_{C_8} d\vec{r} &= \vec{e}_x \int_a^0 dx.
\end{aligned} \tag{82}$$

It is then straightforward to calculate the linking integrals $L(C_i, C_j)$. For notational simplicity let us introduce the following abbreviations

$$\begin{aligned}
L_{ij} &= 4\pi L(C_i, C_j), \\
f(x, y, z) &= (x^2 + y^2 + z^2)^{-3/2}
\end{aligned} \tag{83}$$

Rescaling all coordinates by a , i.e. $x/a \rightarrow x$ etc., we find the explicit expressions

$$\begin{aligned}
L_{14} &= -\int_0^{\frac{b}{a}} dy \int_0^1 dz f(1, y, z), & L_{15} &= -\frac{b}{a} \int_{-1}^1 dx \int_{-1}^1 dz f\left(x, \frac{b}{a}, z\right) \\
L_{16} &= \int_{\frac{b}{a}}^0 dy \int_{-1}^1 dz f(1, y, z), & L_{24} &= \int_0^{-1} dx \int_0^{\frac{b}{a}} dy f(x+1, y, 1), \\
L_{26} &= \int_0^1 dx \int_0^{\frac{b}{a}} dy f(x+1, y, 1), & L_{35} &= \frac{b}{a} \int_0^2 dx \int_0^1 dz f\left(x, \frac{b}{a}, z\right), \\
L_{36} &= 2 \int_0^{\frac{b}{a}} dy \int_0^1 dz f(2, y, z), & L_{47} &= -2 \int_0^{\frac{b}{a}} dy \int_0^{-1} dz f(2, y, z), \\
L_{48} &= -\int_1^0 dx \int_0^{\frac{b}{a}} dy f(x+1, y, 1), & L_{57} &= \frac{b}{a} \int_{-2}^0 dx \int_0^1 dz f\left(x, \frac{b}{a}, z\right),
\end{aligned}$$

$$L_{68} = - \int_{-1}^0 dx \int_0^{b/a} dy f(x, y, 1). \quad (84)$$

Let us first consider the writhing number of the final field configuration at $t = \bar{t}_3$ (see fig. 7) for which $b = a$. In this case all linking integrals can be reduced to the three following integrals

$$\begin{aligned} I &= \int_0^1 dx \int_0^1 dy f(x, y, 1), \\ K &= \int_0^1 dx \int_1^2 dy f(x, y, 1), \\ M &= \int_0^1 dx \int_0^1 dy f(x, y, 2). \end{aligned} \quad (85)$$

One finds

$$\begin{aligned} L_{14} &= -2I, & L_{15} &= -4I, & L_{16} &= -2I, \\ L_{24} &= -I, & L_{26} &= K, & L_{35} &= I + K, & L_{36} &= 2M, \\ L_{47} &= 2M, & L_{48} &= K, & L_{57} &= I + K, & L_{68} &= -I. \end{aligned}$$

With this result the writhing number becomes ($C \equiv C(b = a)$)

$$W(C) = \frac{8}{4\pi} [-2I + K + M]. \quad (86)$$

The integrals I, K, M can be trivially taken by noticing that

$$f(x, y, z) = (x^2 + y^2 + z^2)^{-3/2} = \frac{1}{y^2 + z^2} \frac{d}{dx} \frac{x}{\sqrt{x^2 + y^2 + z^2}}. \quad (87)$$

One finds

$$I = \frac{\pi}{6}, \quad K = \arctan\left(\frac{1}{3}\sqrt{6}\right) - \frac{\pi}{6}, \quad M = \frac{1}{2} \arctan\left(\frac{1}{12}\sqrt{6}\right) \quad (88)$$

so that the writhing number becomes

$$W(C) = -1 + \frac{2}{\pi} \left[\arctan \left(\frac{1}{3} \sqrt{6} \right) + \frac{1}{2} \arctan \left(\frac{1}{12} \sqrt{6} \right) \right]. \quad (89)$$

Using the addition theorem for the arcus-tangent function one eventually finds

$$W(\bar{t}_3) = W(C) = -\frac{1}{2}. \quad (90)$$

The calculation of the writhing number of the vortex configuration at $t = \bar{t}_1$ proceeds completely analogously. The writhing number of the vortex loops at $t = \bar{t}_1$ is still given by eq. (81). Furthermore the line segments C_1, C_2, C_3, C_7 and C_8 are the same for the vortex loops at $t = \bar{t}_3$ and $t = \bar{t}_1$. What is different are the line segments C_4, C_5 and C_6 . The changes of these line segments can be seen to merely change the signs of *all* contributing linking integrals L_{ij} quoted in eq. (84), so that we obtain

$$W(\bar{t}_1) = -W(\bar{t}_3) = \frac{1}{2}. \quad (91)$$

Let us now investigate how the writhing numbers changes at $t = \bar{t}_2$ as C_5 crosses C_1 . There is obviously an intersection point at $(x, y, z) = (0, 0, 0)$ at which $W(C)$ changes by $|\Delta W| = 2$. With the above notation the change in the writhing number at $t = \bar{t}_2$ when C_5 crosses C_1 is given by

$$\Delta W(\bar{t}_2) = \lim_{b \rightarrow 0} [W(C(b)) - W(C(-b))]. \quad (92)$$

Obviously only such linking integrals L_{ij} contribute to $\Delta W(\bar{t}_2)$ (92) which are odd in b and non-vanishing in the limit $b \rightarrow 0$. Since the paths C_4 and C_6 vanish in the limit $b \rightarrow 0$ all linking integrals containing C_4 or C_6 vanish $L(C_4, C_i) = L(C_6, C_i) = 0$ for all i . The remaining non-zero linking integrals are in fact odd in b and we obtain from eq. (81) for the change in the writhing number

$$\begin{aligned} \Delta W(\bar{t}_2) &= 4 \lim_{b \rightarrow 0} [L(C_1, C_5) + L(C_3, C_5) + L(C_5, C_7)] \\ &= \Delta W(\bar{t}_2)^i(0) + \Delta W(\bar{t}_i)^t(-a) + \Delta W(\bar{t}_i)^t(a) \end{aligned} \quad (93)$$

Here the first, second and third terms represent the contributions to the change in the writhing number from the intersection point at $(0, 0, 0)$ and the twisting points at $(-a, 0, 0)$

and $(a, 0, 0)$, respectively. Using the explicit expressions for the linking integrals given in eq. (84) and taking the limit $b \rightarrow 0$ one finds

$$\begin{aligned}\Delta W (\bar{t}_2)^i (0) &= -2, \\ \Delta W (\bar{t}_2)^t (\mp a) &= \frac{1}{2}.\end{aligned}\tag{94}$$

The intersection point changes the writhing number by (-2) while the twisting points change it by $\frac{1}{2}$. The total change of the writhing number at $t = \bar{t}_2$ is then given by

$$\Delta W (\bar{t}_2) = -1.\tag{95}$$

Appendix B: The twist

As a cross check we calculate in the following the twist of the final vortex configuration shown in fig. 7 at $t = \bar{t}_3$, see also fig. 8. Note that due to eq. (58) the sum of the twist and the writhing number has to be integer-valued.

To evaluate the twist we use the same parametrisation of the path as in the evaluation of the writhing number, see Appendix A. Furthermore we use the framing shown in fig. 9. This framing of the path, i.e. $\hat{n}(s)$, does not change along the loop segments C_1, C_2, C_5, C_8 , which hence do not contribute to the twist. At the remaining loop segments the framing is chosen as

$$\begin{aligned}C_3 : \hat{n}(z) &= \vec{e}_y \cos \pi \frac{a-z}{za} - \vec{e}_x \sin \pi \frac{a-z}{2a}, \\ C_4 : \hat{n}(y) &= -\vec{e}_x \cos \frac{\pi y}{2a} + \vec{e}_z \sin \frac{\pi y}{2a}, \\ C_6 : \hat{n}(y) &= \vec{e}_z \sin \frac{\pi y}{2a} - \vec{e}_x \cos \frac{\pi y}{2a}, \\ C_7 : \hat{n}(z) &= -\vec{e}_x \cos \frac{\pi z}{za} - \vec{e}_y \sin \frac{\pi z}{2a}.\end{aligned}\tag{96}$$

Straightforward evaluation of the twist integrals yields the following results

$$\begin{aligned}T(C_3, \hat{n}) &= -\frac{1}{4}, T(C_4, \hat{n}) = \frac{1}{4}, \\ T(C_6, \hat{n}) &= \frac{1}{4}, T(C_7, \hat{n}) = \frac{1}{4}.\end{aligned}\tag{97}$$

The total twist of the vortex loop at $t = \bar{t}_3$ is then given by

$$\begin{aligned}T(C(\bar{t}_3)) &= T(C_3, \hat{n}) + T(C_4, \hat{n}) + T(C_6, \hat{n}) + T(C_7, \hat{n}) \\ &= -\frac{1}{4} + \frac{1}{4} + \frac{1}{4} + \frac{1}{4} = \frac{1}{2}.\end{aligned}\tag{98}$$

References

- [1] G. 't Hooft, Nucl. Phys. **B138** (1978) 1;
 Y. Aharonov, A. Casher and S. Yankielowicz, Nucl. Phys. **B146** (1978) 256;
 J. M. Cornwall, Nucl. Phys. **B157** (1979) 392
 G. Mack and V. B. Petkova, Ann. Phys. (NY) **123** (1979) 442;
 G. Mack, Phys. Rev. Lett. **45** (1980) 1378;
 G. Mack and V. B. Petkova, Ann. Phys. (NY) **125** (1989) 117;
 G. Mack, in: *Recent Developments in Gauge Theories*, eds. G. 't Hooft et al.
 (Plenum, New York, 1980);
 G. Mack and E. Pietarinen, Nucl. Phys. **B205** [FS5] (1982) 141
 H. B. Nielsen and P. Olesen, Nucl. Phys. **B160** (1979) 380;
 H. Ambjørn and P. Olesen, Nucl. Phys. **B170** [FS1] (1980) 60;
 J. J. Ambjørn and P. Olesen, Nucl. Phys. **B170** [FS1] (1980) 265;
 E. T. Tomboulis, Phys. Rev. **D 23** (1981) 2371
- [2] Del Debbio, M. Faber, J. Greensite, Š. Olejnik, Phys. Rev. **D55** (1997) 2298
- [3] K. Langfeld, H. Reinhardt, O. Tennert, Phys. Lett. **B419** (1998) 317
- [4] L. Del Debbio, M. Faber, J. Giedt, J. Greensite and Š. Olejnik, Phys. Rev. **D 58**
 (1998) 094501
- [5] K. Langfeld, O. Tennert, M. Engelhardt and H. Reinhardt, Phys. Lett. **B542** (1999)
 301, M. Engelhardt, K. Langfeld, H. Reinhardt and O. Tennert, Phys. Rev. **D61**
 (2000) 054504
- [6] T. G. Kovacs, E. T. Tomboulis, Phys. Rev. Lett. **85** (2000) 704
- [7] P. de Forcrand and M. D'Elia, Phys. Rev. Lett. **82** (1999) 4582.
- [8] M. Engelhardt, H. Reinhardt, Nucl. Phys. **B567** (2000) 249
- [9] H. Reinhardt, M. Engelhardt, Proceedings of the XVIII Lisbon Autumn School,
 "Topology of Strongly Correlated Systems", Lisbon, 8-13 October, 2000, hep-
 th/0010031
- [10] J. M. Cornwall, Phys. Rev. **D61** (2000) 085012

- [11] M. Engelhardt and H. Reinhardt, Nucl. Phys. **B585** (2000) 591
- [12] M. Engelhardt, Nucl. Phys. **B585** (2000) 614
- [13] R. Bertle, M. Engelhardt, M. Faber, Phys. Rev. **D64** (2001) 074504
- [14] M. Faber, J. Greensite, Š. Olejnik, Phys. Rev. **D57** (1998) 2603
- [15] K. Langfeld, H. Reinhardt, M. Quandt, hep-th/9610213
- [16] H. Reinhardt, Nucl. Phys. **B503** (1997) 505
- [17] R. Bertle, M. Faber, J. Greensite. Š. Olejnik, JHEP **9903** (1999) 019
- [18] L. Del Debbio. M. Faber, J. Greensite and Š. Olejnik, in: *New Developments in Quantum Field Theory*, eds. P. H. Damgaard and J. Jurkiewicz (Plenum Press, New York - London, 1998); hep-lat/9708023

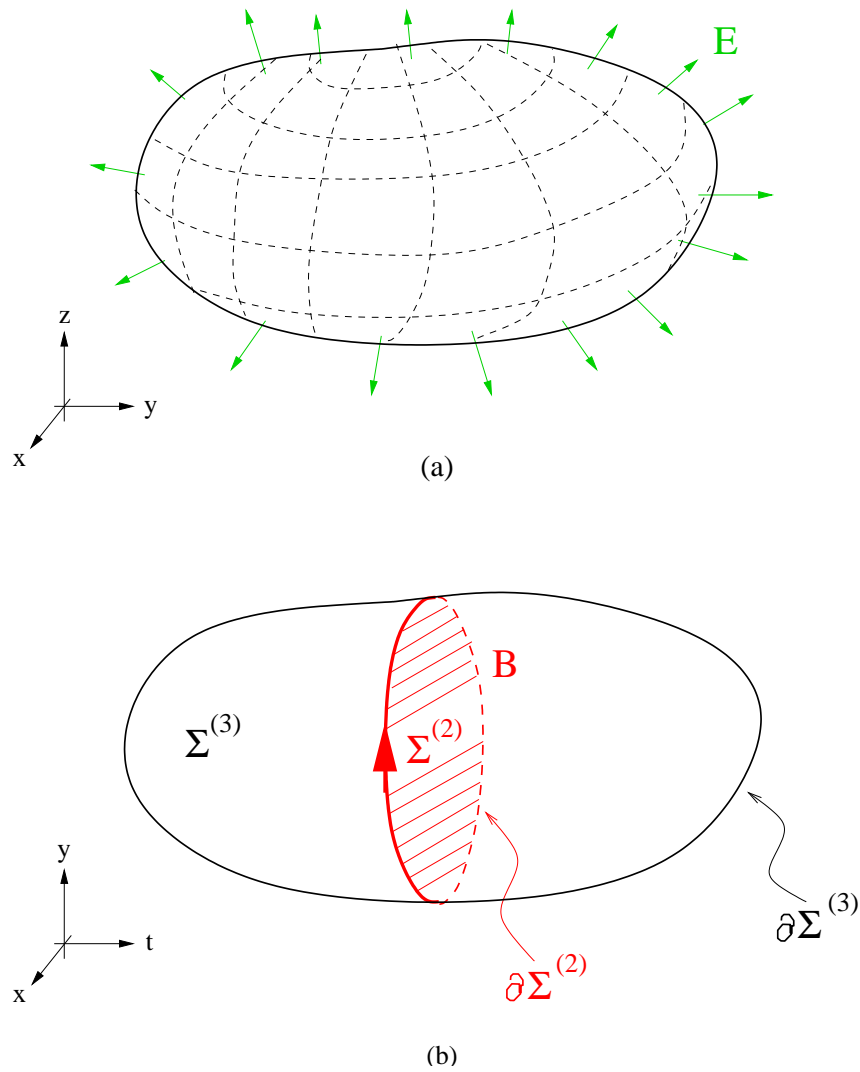
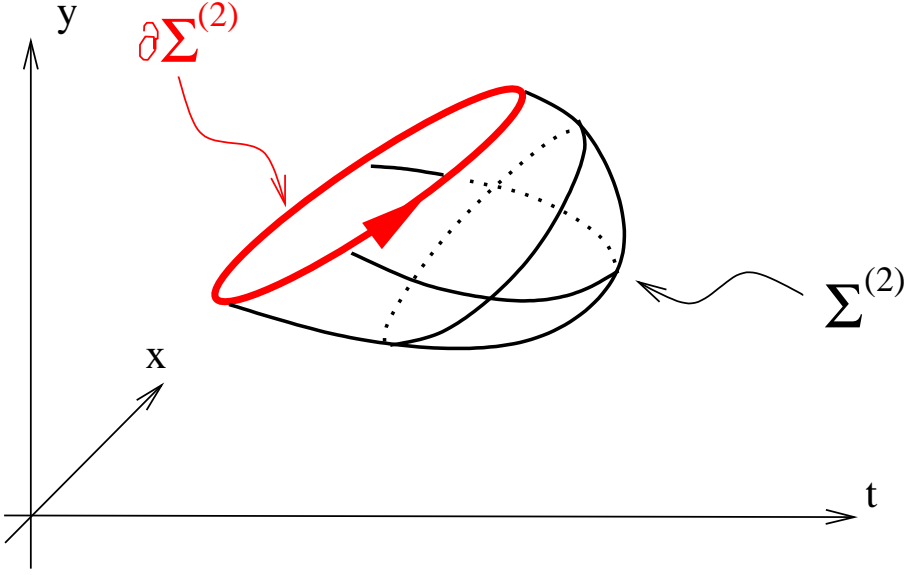
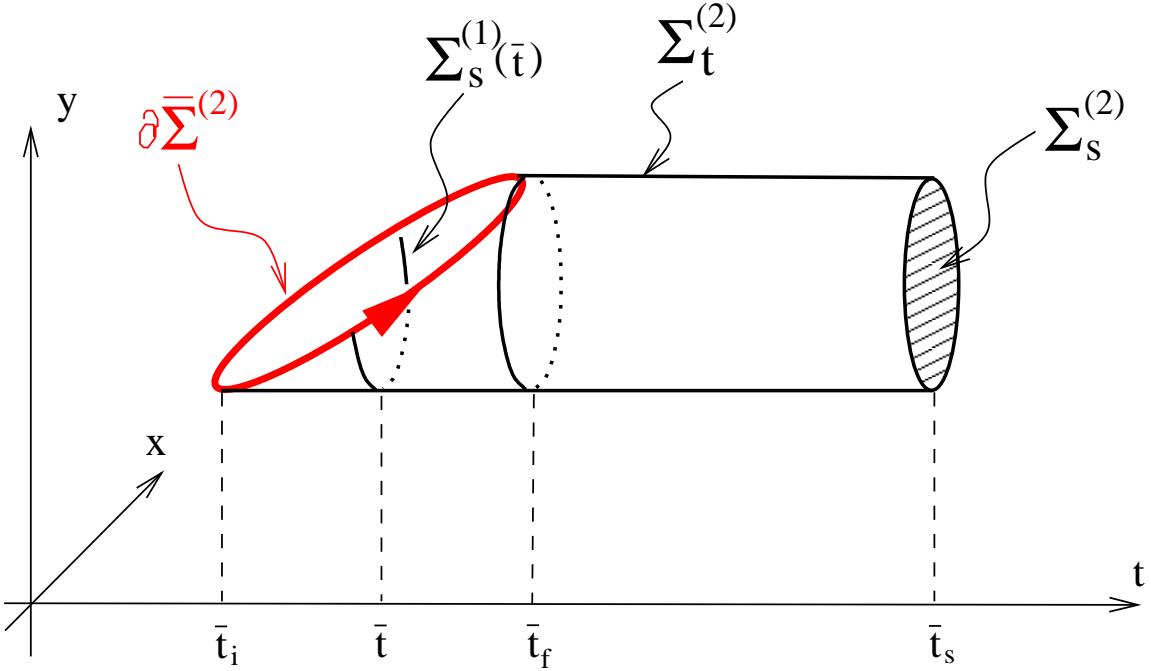


Figure 1: Illustration of (a) a (non-generic) electric center vortex and (b) a magnetic center vortex in ordinary 3-space. While the electric vortex sheet (a) exists only at a single time-instant the magnetic vortex (b) evolves in time.



(a)



(b)

Figure 2: (a) Illustration of a mathematically idealised center vortex loop $\partial\Sigma^{(2)}$ as boundary of an open 2-dimensional surface $\Sigma^{(2)}$, which is neither temporal nor spatial. (b) The same vortex loop $\partial\Sigma^{(2)}$ but with a different hypersurface $\bar{\Sigma}^{(2)} = \Sigma_t^{(2)} + \Sigma_s^{(2)}$, which has been chosen as the surface of an open cylinder whose mantle Σ_t is temporal while its face Σ_s is spatial. Also shown are fixed time \bar{t} slices, where $\Sigma_t^{(2)}$ appears either as an open string ($\bar{t}_i < \bar{t} < \bar{t}_f$) whose boundary points represent the vortex or as a closed string ($\bar{t}_i < \bar{t} < \bar{t}_s$) in the absence of a vortex.

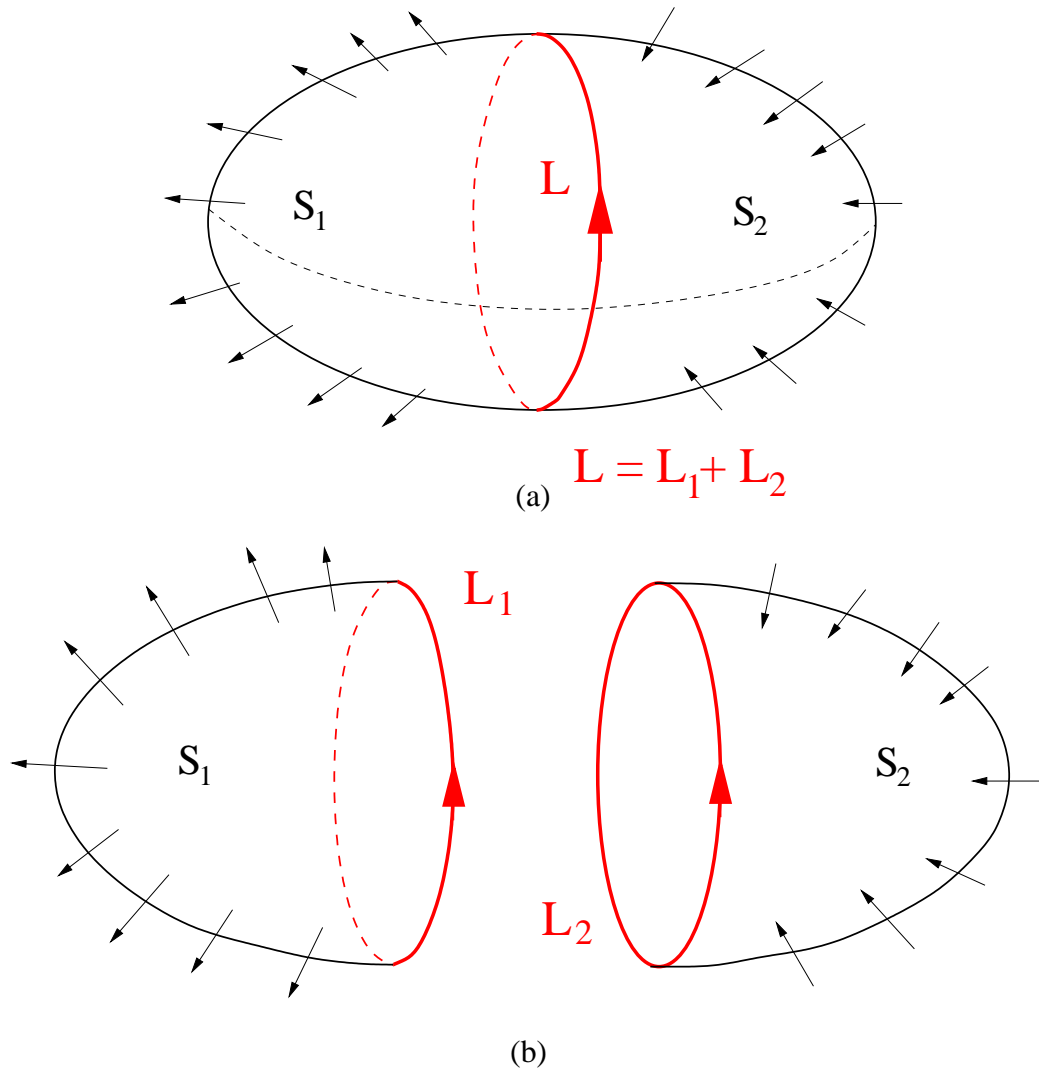


Figure 3: (a) Non-oriented vortex sheet consisting of two oppositely oriented vortex patches S_1 and S_2 joined by a magnetic Dirac monopole. (b) The non-oriented vortex sheet can be considered as arising by glueing together two open oriented vortex patches S_1 and S_2 bounded by center monopole loops L_1 and L_2 , respectively, which add up to a Dirac monopole loop $L = L_1 + L_2$ on the non-oriented vortex shown in (a). Note that S_2 can be considered as a deformation of S_1 which turns the inside of S_1 into the outside of S_2 . This explains why S_1 and S_2 are bounded by identical (center) monopole loops, although they have opposite orientation.

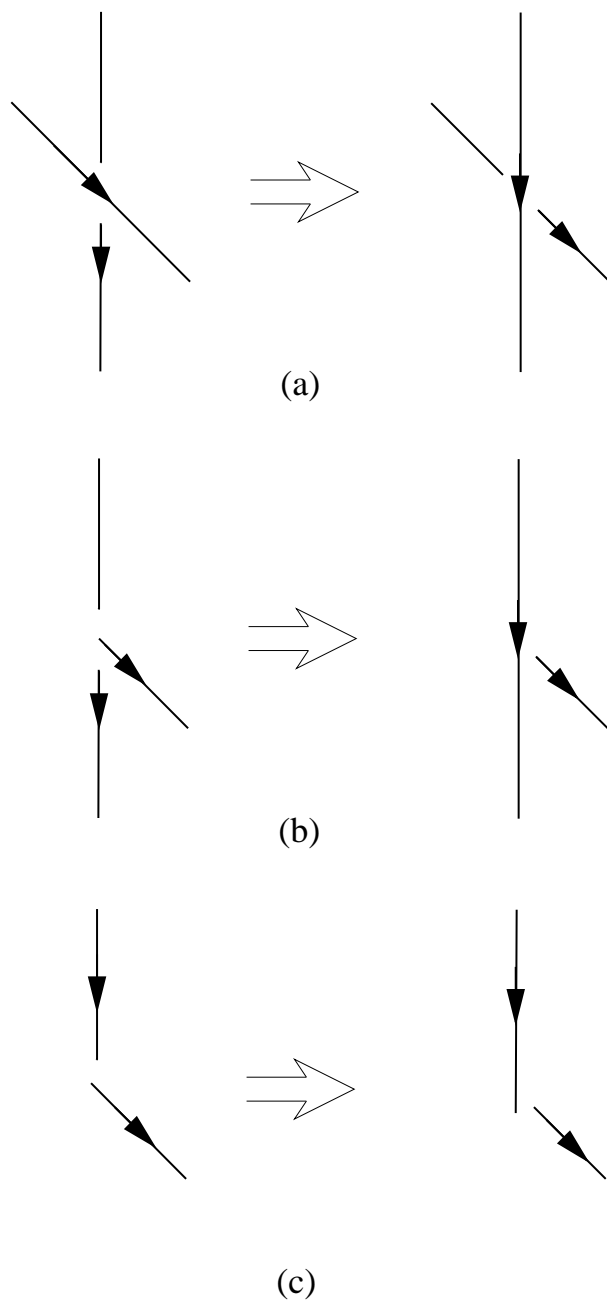


Figure 4: Crossing of (a) two (full) line segments, (b) a full and a half-line and (c) two half-line segments of a closed loop changing the writhing of the loop by $\Delta W = 2$, $\Delta W = 1$ and $\Delta W = \frac{1}{2}$, respectively.

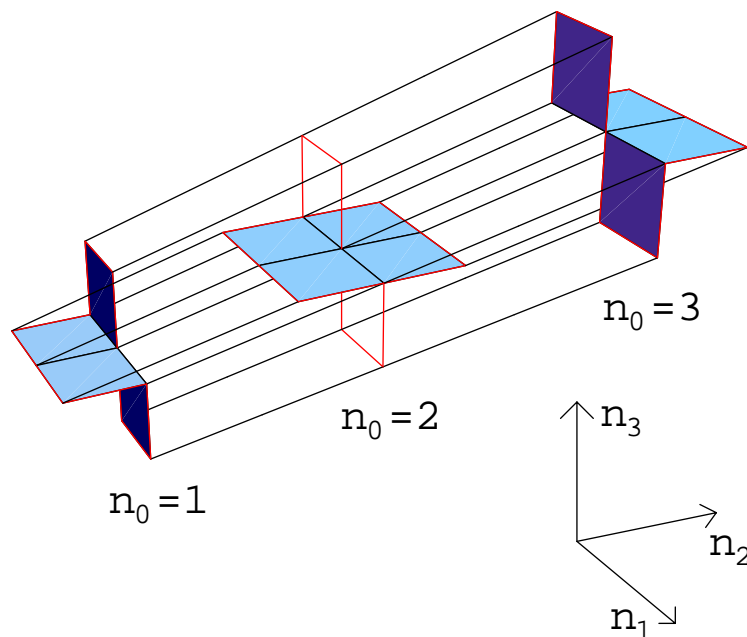


Figure 5: Sample vortex surface configuration taken from [12]. At each lattice time $t = n_0 a$ (a -lattice spacing), shaded plaquettes are part of the vortex surface. These plaquettes are furthermore connected to plaquettes running in time direction; their location can be inferred most easily by keeping in mind that each link of the configuration is connected to exactly two plaquettes (i.e. the surface is closed and contains no intersection lines). Note that the two non-shaded plaquettes at $n_0 = 2$ are *not* part of the vortex; only the two sets of three links bounding them are. These are slices at $n_0 = 2$ of surface segments running in time direction from $n_0 = 1$ through to $n_0 = 3$. Sliced at $n_0 = 2$, these surface segments show up as lines. Furthermore, by successively assigning orientations to all plaquettes, one can convince oneself that the configuration is orientable. The vortex image was generated by means of a MATHEMATICA routine provided by R. Bertle and M. Faber.

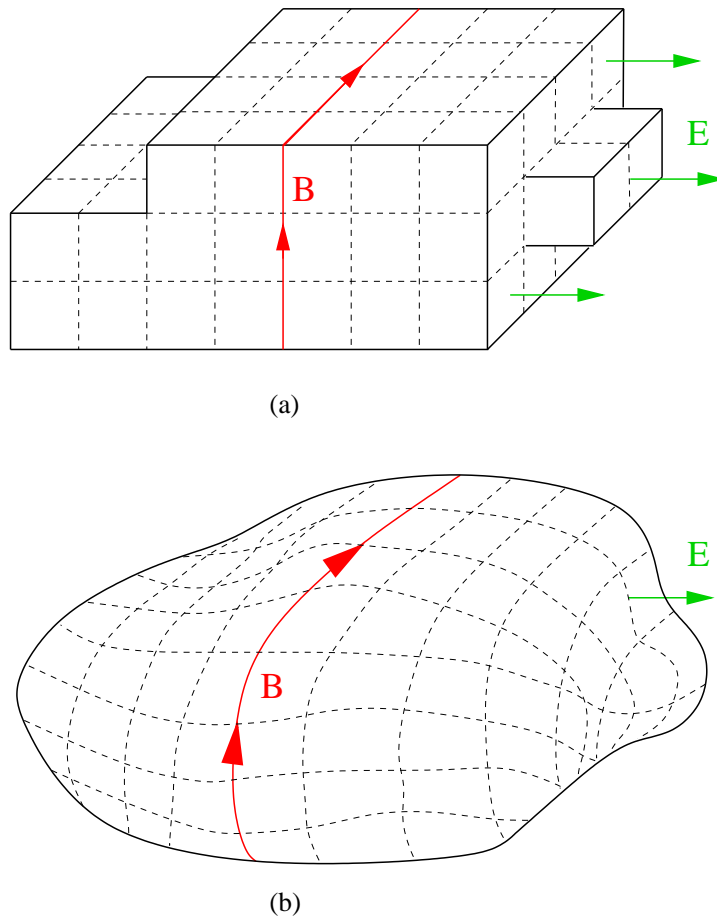


Figure 6: (a) Lattice realization of the smooth continuum center vortex configuration shown in (b). The use of discrete time intervals on the lattice gives rise to purely spatial vortex surface patches, which should be considered as lattice artifacts.

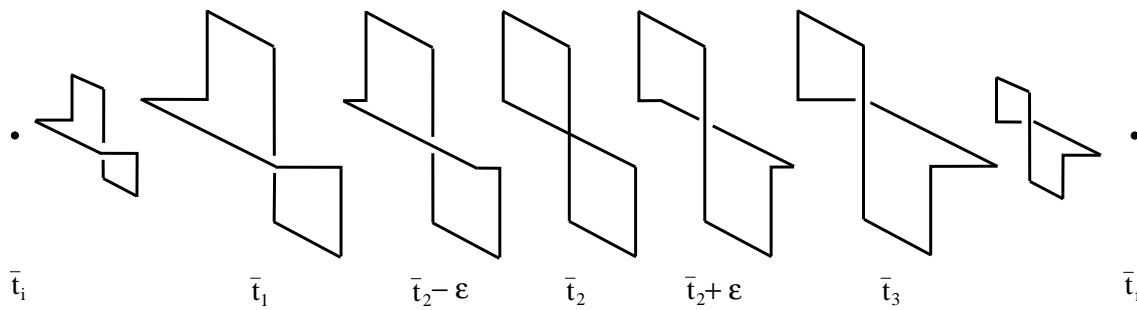


Figure 7: Snap shots at characteristic time instants of the continuum center vortex loop whose lattice realization is shown in 5.

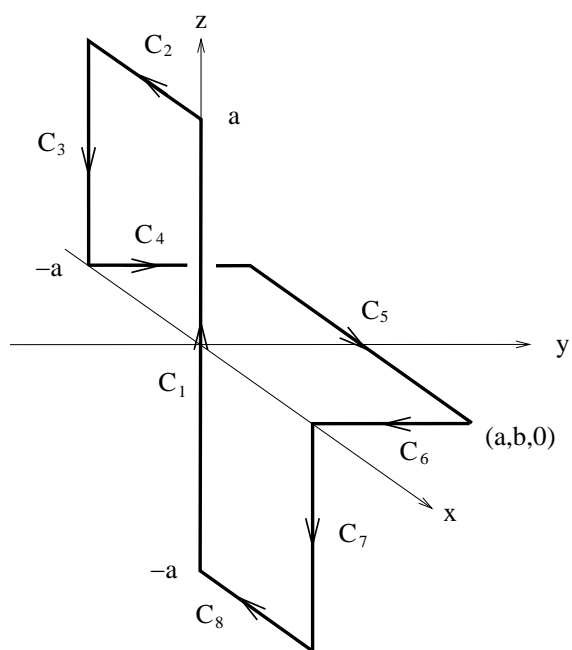


Figure 8: Definition of the line-segments C_i used in the calculation of the writhing number and twist of the vortex loop at $t = \bar{t}_3$ shown in fig. 7.

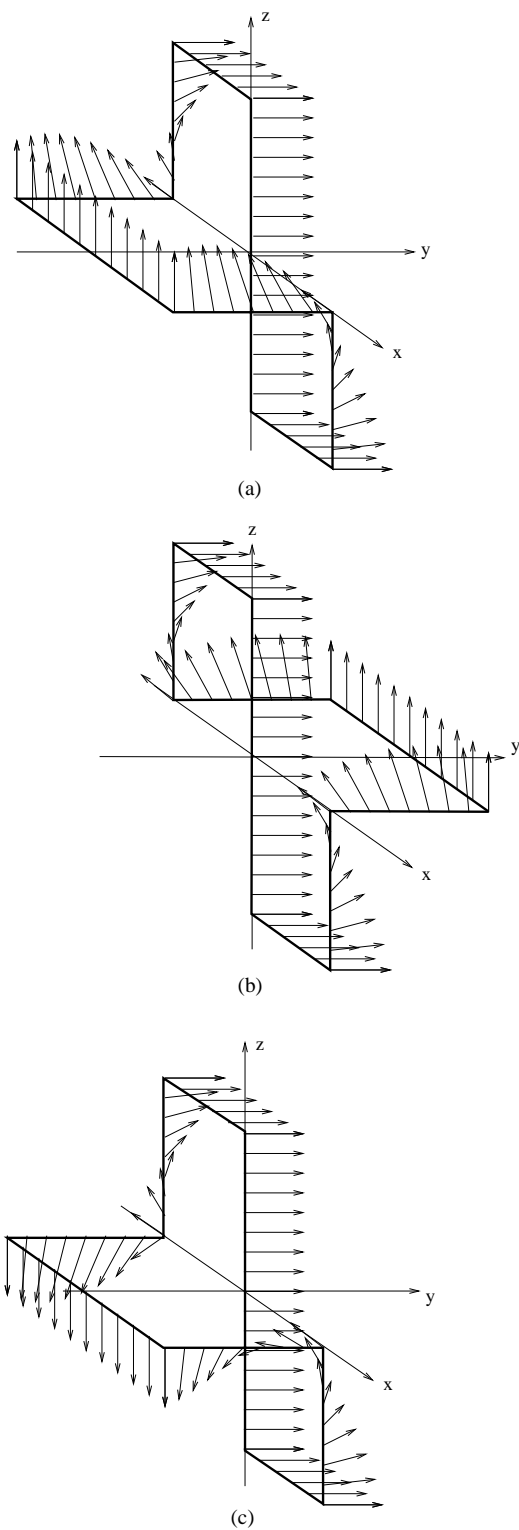


Figure 9: Framings of the vortex loop shown in fig. 7; (a) and (b) show framings of the vortex loop at $t = \bar{t}_1$ and $t = \bar{t}_3$, respectively, with vanishing self-linking number, $SL(C) = 0$. (c) framing of the vortex loop at $t = \bar{t}_1$ with $SL(C) = 1$.

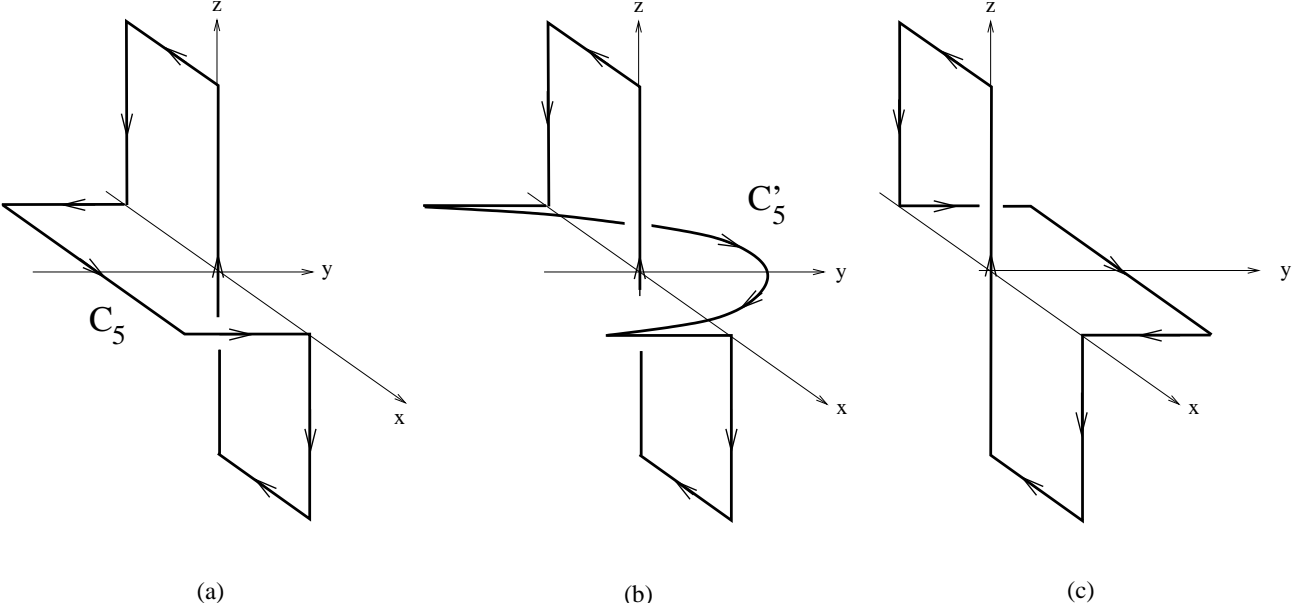


Figure 10: (a) The vortex loop of Fig. 7 at time $t = \bar{t}_1$ (b) shows the same loop as in (a) except that the line-segment C_5 has been deformed to the line-segments C'_5 thereby intersecting the line-segment C_1 . (c) The vortex loop of Fig. 7 at time $t = \bar{t}_3$.

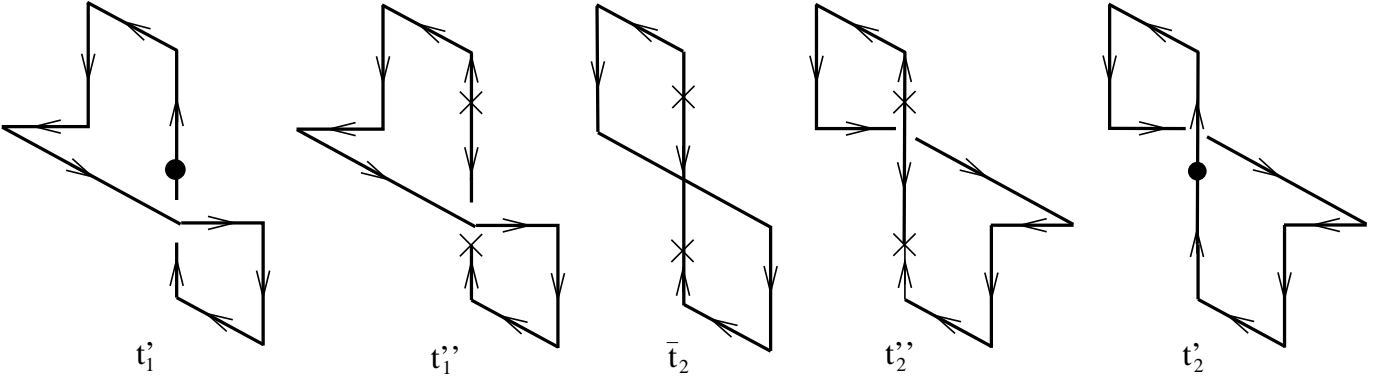


Figure 11: Snap shots at characteristic time instants of the continuum center vortex loop whose lattice realization is obtained from the center vortex configuration shown in fig. 5 if a magnetic monopole loop is added in the $n_0 - n_3$ -plane around the point $(n_0, n_1, n_2, n_3) = (2, 0, 0, 0)$. The crosses denote the positions of the monopole and anti-monopole. The fat dots indicate the creation and annihilation of a monopole-anti-monopole pair.